# Relativistic many-body calculations of energies for doubly-excited $1s2l2l'$ and $1s3l3l'$ states in Li-like ions

**U.I. Safronova and M.S. Safronova**

**Abstract**: Energies of $1s2l2l'$ and $1s3l3l'$ states for Li-like ions with $Z = 6$–100 are evaluated to second order in relativistic many-body perturbation theory. Second-order Coulomb and Breit–Coulomb interactions are included. The calculations start with a Dirac potential and include all possible $1s2l2l'$ and $1s3l3l'$ configurations. Correction for the frequency dependence of the Breit interaction is taken into account in lowest order. The Lamb-shift correction to the energies is also included in lowest order. A detailed discussion of the various contributions to the energy levels is given for Li-like iron ($Z = 26$). We found that the three-electron corrections to the energy contribute about 10–20% of the total second-order energy. Comparisons are made with available experimental data and excellent agreement for term splitting is obtained even for low-$Z$ ions. These calculations are presented as a theoretical benchmark for comparison with experiment and theory.

PACS Nos.: 32.30.Rj, 32.70.Cs, 31.25.Jf, 31.15.Md

**Résumé** : Nous utilisons la théorie relativiste des perturbations au deuxième ordre pour évaluer les énergies des états $1s2l2l'$ et $1s3l3l'$ des ions de type Li avec $Z = 6$–100. Nous incluons les effets de Coulomb et de Breit–Coulomb au deuxième ordre. Le calcul démarre avec un potentiel de Dirac et inclut toutes les configurations possibles $1s2l2l'$ et $1s3l3l'$. Nous tenons compte à l'ordre le plus bas des corrections pour la dépendance en fréquence de l'interaction de Breit. Nous analysons en détail les différentes contributions aux niveaux d'énergie pour le cas $Z = 26$. Nous trouvons que les corrections à trois électrons contribuent à peu près 10–20% du total des corrections de deuxième ordre. Nous comparons nos résultats avec des données expérimentales et trouvons un excellent accord pour la séparation entre états, même pour les ions de faible $Z$. Ces résultats seront utilisés comme barème pour comparaison avec la théorie et l'expérience.

[Traduit par la Rédaction]

Received 30 April 2004. Accepted 7 July 2004. Published on the NRC Research Press Web site at http://cjp.nrc.ca/ on 23 August 2004.

**U.I. Safronova.**[1] Physics Department, University of Nevada, Reno, NV 89557, USA.
**M.S. Safronova.** Department of Physics and Astronomy, 223 Sharp Laboratory, University of Delaware, Newark, DE 19716, USA.

[1]Corresponding author (e-mail: usafrono@nd.edu).

 doi: 10.1139/P04-041 

## 1. Introduction

Excitation energies, nonradiative, and electric dipole (E1) radiative rates for $1s2lnl'$ states along the lithium isoelectronic sequence have been studied theoretically and experimentally during the past 30–40 years. $Z$-expansion [1–3], configuration interaction (CI) [4], multiconfiguration Hartree–Fock (MCHF) [5–7], and multiconfiguration Dirac–Fock (MCDF) [8–10] methods have been used to calculate these quantities for Li-like ions. Comparison of results for Li-like Fe, Ca, and S obtained by different codes is presented by Kato et al. in ref. 11. It should be noted that doubly-excited $1snln'l'$ states give the simplest example of states to study the contribution of correlation energy. There are no filled subshells and any codes based on the Hartree–Fock approximation are not applicable. The second-order perturbation theory describes the correlation effects by including virtual excitations. This contribution can be partly taken into account using the CI method. CI calculations give very accurate results for two-electron systems. The importance of a three-electron interaction for a three-electron system is shown in refs. 12 and 13 for boronlike and aluminumlike systems, respectively. Two-particle and three-particle second-order contributions for $1s2l2l'$ states are given in the nonrelativistic approximation in refs. 1 and 2.

In the present paper, relativistic many-body perturbation theory (RMBPT) is used to determine the $1s2l2l'$–$1s^22l$ and $1s3l3l'$–$1s^23l$ transition energies in Li-like ions with nuclear charges $Z = 6$–$100$. We illustrate our calculation with detailed studies of the case of Li-like iron, $Z = 26$. Our calculations are carried out to second order in perturbation theory and include the second-order Coulomb and Breit interactions. Correction for the frequency-dependent Breit interaction is taken into account in the lowest order. The screened self-energy and vacuum polarization data given by Johnson and Soff [14] are used to determine the quantum-electrodynamic (QED) correction $E^{(\mathrm{Lamb})}$. Three-electron contributions to the energy are compared with the two-electron contributions and are found to contribute about 20–30% of the total second-order energy.

Our perturbation theory calculations are carried out using single-particle orbitals calculated in the Dirac potential. As a first step, we determine and store the 28 $1s2l$ and $2l2l'$, and 171 $1s3l$ and $3l3l'$ two-particle matrix elements of the effective Hamiltonian, $\langle nln'l'\ J|H^{\mathrm{eff}}|nl''n'l'''\ J\rangle$, calculated in the first and second orders. It should be noted that these one- and two-particle matrix elements could be used also to evaluate energies of the $(nln'l')$ levels for heliumlike ions. Finally, second-order three-particle matrix elements are evaluated. Combining these data using the method described below, we calculate the two- and three-particle contributions to the energies of Li-like ions.

The present calculations are compared with data recommended by the National Institute of Standards and Technology (NIST) from refs. 15–31. Comparisons of multiplet splitting for ions along the isoelectronic sequence with available experimental data are also given.

## 2. Method

The evaluation of the second-order energies for doubly-excited states in Li-like ions follows the pattern of the corresponding calculation for B-like ions given in ref. 12. In particular, we calculate the second-order two-particle matrix elements for He-like ions, and recouple them as described in the Appendix, to obtain the contributions from all diagrams of the type shown in Fig. 1*b*. We discuss in the Appendix how these matrix elements are combined to obtain the two-particle contributions to energies of Li-like ions. Intrinsically, three-particle diagrams of the type shown in Fig. 1*c* also contribute to the second-order energy for Li-like ions. We discuss the evaluation of these three-particle diagrams in detail in the Appendix. It should be noted that the three-particle matrix elements calculated here can also be used in calculations of energies of ions with four or more valence electrons.

The model space for $1s2l2l'$ states of Li-like ions includes seven odd-parity states consisting of three $J = 1/2$ states, three $J = 3/2$ states, and one $J = 5/2$ state. There are nine $1s2l2l'$ even-parity states consisting of four $J = 1/2$ states, three $J = 3/2$ states, and two $J = 5/2$ states. The model space

**Fig. 1.** First-order (1E) and second-order (2E and 2G) diagrams. The broken lines designate Coulomb + Breit interactions and continuous lines are electrons in different states.

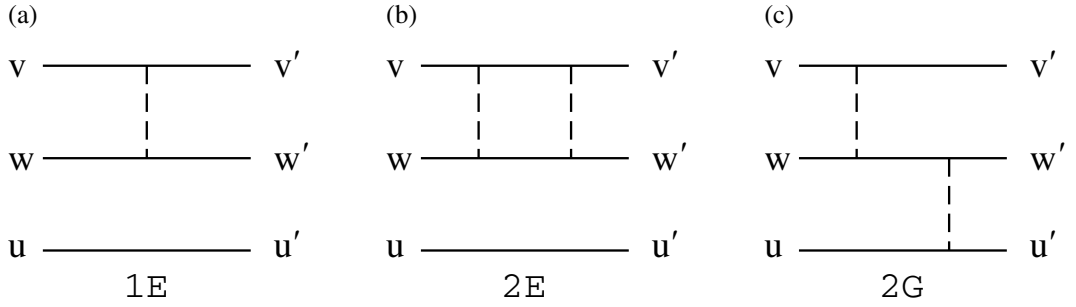


for $1s3l3l'$ states of Li-like ions includes thirty odd-parity states consisting of seven $J = 1/2$ states, ten $J = 3/2$ states, eight $J = 5/2$ states, four $J = 7/2$ states, and one $J = 9/2$ state. There are thirty-three $1s3l3l'$ even-parity states consisting of eight $J = 1/2$ states, ten $J = 3/2$ states, nine $J = 5/2$ states, four $J = 7/2$ states, and two $J = 9/2$ states. The distribution of the sixteen $1s2l2l'$ and sixty-three $1s3l3l'$ states in the model space is summarized in Table 1 where both $jj$ and LS designations are given.

### 2.1. Energy matrix elements

In Table 2, we give various contributions to the second-order energies for the special case of doubly-excited $1s2l2l'$ states in Li-like iron, $Z = 26$. In Table 2, we show the two-body and three-body second-order Coulomb and Breit contributions to the energy matrix labeled $E_2^{(2)}$, $E_3^{(2)}$ and $B_2^{(2)}$, $B_3^{(2)}$, respectively. The expressions for $E_2^{(2)}$ and $E_3^{(2)}$ are given by (A5), (A7), and (A11). The same expressions for $B_2^{(2)}$ and $B_3^{(2)}$ are obtained from the expressions for $E_2^{(2)}$ and $E_3^{(2)}$ replacing one Coulomb matrix element by a Breit matrix element (see (A12)). There are sixteen diagonal and twenty-four nondiagonal matrix elements for $2l2l'(J_1)1s[J]$ three-particle states in $jj$ coupling. It can be seen from Table 2 that the Coulomb three-body contributions are almost half of the Coulomb two-body contributions. The Breit $B_i^{(2)}$ matrix elements are smaller than the Coulomb $E_i^{(2)}$ matrix elements by a factor of 100 for many cases. The values of the nondiagonal contributions are smaller than the values of the diagonal contributions by a factor of 3–10.

In Figs. 2*a* and 2*b*, we present two-particle ($E_2^{(2)}$ and $B_2^{(2)}$) and three-particle ($E_3^{(2)}$ and $B_3^{(2)}$) contributions for the $2s_{1/2}2p_{3/2}(2)1s[5/2]$ diagonal matrix element as functions of $Z$. We see from Fig. 2*a* that the ratio $E_3^{(2)}/E_2^{(2)}$ is equal to 1/2 and is almost constant for all $Z$; however, the ratio of $B_3^{(2)}/B_2^{(2)}$ decreases with the increase in $Z$.

Reference 33 shows that the leading term for $E_2^{(2)}$ is independent of $Z$ and the leading term for $B_2^{(2)}$ is proportional to $(\alpha Z)^2$.

$$E_2^{(2)} = E_{20} + Z^2\alpha^2 E_{22} + Z^4\alpha^4 E_{24} + \cdots \tag{1}$$

$$B_2^{(2)} = Z^2\alpha^2 B_{22} + Z^4\alpha^4 B_{24} + \cdots \tag{2}$$

The nonrelativistic second-order term $E_{20}$ was given in refs. 1 and 2 for doubly-excited $1s2l2l'$ states. Comparing those values with $E_2^{(2)}$, we can estimate the next term in (1). For example, for the diagonal matrix element presented in Fig. 2*a* we obtain

$$E_2^{(2)}(a,a) = -0.0148094 - 0.096Z^2\alpha^2 + \cdots \tag{3}$$

**Table 1.** Possible doubly excited $2l2l'1s$ and $3l3l'1s$ states of Li-like ions in $jj$ and LS coupling schemes.

| Even-parity states | | Odd-parity states | |
|---|---|---|---|
| $jj$ coupling | LS coupling | $jj$ coupling | LS coupling |
| $2s_{1/2}2s_{1/2}(0)1s$ | $2s^2(^1S)1s\ ^2S_{1/2}$ | $2s_{1/2}2p_{1/2}(0)1s$ | $2s2p(^3P)1s\ ^4P_{1/2}$ |
| $2p_{1/2}2p_{1/2}(0)1s$ | $2p^2(^3P)1s\ ^4P_{1/2}$ | $2s_{1/2}2p_{1/2}(1)1s$ | $2s2p(^3P)1s\ ^2P_{1/2}$ |
| $2p_{3/2}2p_{3/2}(0)1s$ | $2p^2(^3P)1s\ ^2P_{1/2}$ | $2s_{1/2}2p_{3/2}(1)1s$ | $2s2p(^1P)1s\ ^2P_{1/2}$ |
| $2p_{1/2}2p_{3/2}(1)1s$ | $2p^2(^1S)1s\ ^2S_{1/2}$ | | |
| | | $2s_{1/2}2p_{1/2}(1)1s$ | $2s2p(^3P)1s\ ^4P_{3/2}$ |
| $2p_{1/2}2p_{3/2}(1)1s$ | $2p^2(^3P)1s\ ^4P_{3/2}$ | $2s_{1/2}2p_{3/2}(1)1s$ | $2s2p(^3P)1s\ ^2P_{3/2}$ |
| $2p_{1/2}2p_{3/2}(2)1s$ | $2p^2(^1D)1s\ ^2D_{3/2}$ | $2s_{1/2}2p_{3/2}(2)1s$ | $2s2p(^1P)1s\ ^2P_{3/2}$ |
| $2p_{3/2}2p_{3/2}(2)1s$ | $2p^2(^3P)1s\ ^2P_{3/2}$ | | |
| | | $2s_{1/2}2p_{3/2}(2)1s$ | $2s2p(^1P)1s\ ^4P_{5/2}$ |
| $2p_{1/2}2p_{3/2}(2)1s$ | $2p^2(^3P)1s\ ^4P_{5/2}$ | | |
| $2p_{3/2}2p_{3/2}(2)1s$ | $2p^2(^3P)1s\ ^2D_{5/2}$ | | |
| $3s_{1/2}3s_{1/2}(0)1s$ | $3s^2(^1S)1s\ ^2S_{1/2}$ | $3s_{1/2}3p_{1/2}(0)1s$ | $3s3p(^3P)1s\ ^4P_{1/2}$ |
| $3s_{1/2}3d_{3/2}(1)1s$ | $3p^2(^3P)1s\ ^4P_{1/2}$ | $3s_{1/2}3p_{1/2}(1)1s$ | $3s3p(^3P)1s\ ^2P_{1/2}$ |
| $3p_{1/2}3p_{1/2}(0)1s$ | $3s3d(^3D)1s\ ^4D_{1/2}$ | $3s_{1/2}3p_{3/2}(1)1s$ | $3s3p(^1P)1s\ ^2P_{1/2}$ |
| $3p_{1/2}3p_{3/2}(1)1s$ | $3p^2(^3P)1s\ ^2P_{1/2}$ | $3p_{1/2}3d_{3/2}(1)1s$ | $3p3d(^3D)1s\ ^4D_{1/2}$ |
| $3p_{3/2}3p_{3/2}(0)1s$ | $3p^2(^1S)1s\ ^2S_{1/2}$ | $3p_{3/2}3d_{3/2}(0)1s$ | $3p3d(^3P)1s\ ^4P_{1/2}$ |
| $3d_{3/2}3d_{3/2}(0)1s$ | $3d^2(^3P)1s\ ^4P_{1/2}$ | $3p_{3/2}3d_{3/2}(1)1s$ | $3p3d(^3P1s\ ^2P_{1/2}$ |
| $3d_{3/2}3d_{5/2}(1)1s$ | $3d^2(^3P)1s\ ^2P_{1/2}$ | $3p_{3/2}3d_{5/2}(1)1s$ | $3p3d(^1P)1s\ ^2P_{1/2}$ |
| $3d_{5/2}3d_{5/2}(0)1s$ | $3d^2(^1S)1s\ ^2S_{1/2}$ | | |
| | | $3s_{1/2}3p_{1/2}(1)1s$ | $3s3p(^3P)1s\ ^4P_{3/2}$ |
| $3s_{1/2}3d_{3/2}(1)1s$ | $3s3d(^3D)1s\ ^2D_{3/2}$ | $3s_{1/2}3p_{3/2}(1)1s$ | $3s3p(^3P)1s\ ^2P_{3/2}$ |
| $3s_{1/2}3d_{3/2}(2)1s$ | $3p^2(^3P)1s\ ^4P_{3/2}$ | $3s_{1/2}3p_{3/2}(2)1s$ | $3s3p(^1P)1s\ ^2P_{3/2}$ |
| $3s_{1/2}3d_{5/2}(2)1s$ | $3s3d(^3D)1s\ ^4D_{3/2}$ | $3p_{1/2}3d_{3/2}(1)1s$ | $3p3d(^3F)1s\ ^4F_{3/2}$ |
| $3p_{1/2}3p_{3/2}(1)1s$ | $3s3d(^1D)1s\ ^2D_{3/2}$ | $3p_{1/2}3d_{3/2}(2)1s$ | $3p3d(^3D)1s\ ^2D_{3/2}$ |
| $3p_{1/2}3p_{3/2}(2)1s$ | $3p^2(^3P)1s\ ^2P_{3/2}$ | $3p_{1/2}3d_{5/2}(2)1s$ | $3p3d(^3D)1s\ ^4D_{3/2}$ |
| $3p_{3/2}3p_{3/2}(2)1s$ | $3p^2(^1D1s\ ^2D_{3/2}$ | $3p_{3/2}3d_{3/2}(1)1s$ | $3p3d(^3P)1s\ ^4P_{3/2}$ |
| $3d_{3/2}3d_{3/2}(2)1s$ | $3d^2(^3F)1s\ ^4F_{3/2}$ | $3p_{3/2}3d_{3/2}(2)1s$ | $3p3d(^1D)1s\ ^2D_{3/2}$ |
| $3d_{3/2}3d_{5/2}(1)1s$ | $3d^2(^3P)1s\ ^4P_{3/2}$ | $3p_{3/2}3d_{5/2}(1)1s$ | $3p3d(^3P1s\ ^2P_{3/2}$ |
| $3d_{3/2}3d_{5/2}(2)1s$ | $3d^2(^3P)1s\ ^2P_{3/2}$ | $3p_{3/2}3d_{5/2}(2)1s$ | $3p3d(^1P)1s\ ^2P_{3/2}$ |
| $3d_{5/2}3d_{5/2}(2)1s$ | $3d^2(^1D)1s\ ^2D_{3/2}$ | | |
| | | $3s_{1/2}3p_{3/2}(2)1s$ | $3s3p(^3P)1s\ ^4P_{5/2}$ |
| $3s_{1/2}3d_{3/2}(2)1s$ | $3s3d(^3D)1s\ ^2D_{5/2}$ | $3p_{1/2}3d_{3/2}(2)1s$ | $3p3d(^3F)1s\ ^4F_{5/2}$ |
| $3s_{1/2}3d_{5/2}(2)1s$ | $3p^2(^3P)1s\ ^4P_{5/2}$ | $3p_{1/2}3d_{5/2}(2)1s$ | $3p3d(^3D)1s\ ^2D_{5/2}$ |
| $3s_{1/2}3d_{5/2}(3)1s$ | $3s3d(^3D)1s\ ^4D_{5/2}$ | $3p_{1/2}3d_{5/2}(3)1s$ | $3p3d(^3F)1s\ ^2F_{5/2}$ |
| $3p_{1/2}3p_{3/2}(2)1s$ | $3s3d(^1D)1s\ ^2D_{5/2}$ | $3p_{3/2}3d_{3/2}(2)1s$ | $3p3d(^3D)1s\ ^4D_{5/2}$ |
| $3p_{3/2}3p_{3/2}(2)1s$ | $3p^2(^1D)1s\ ^2D_{5/2}$ | $3p_{3/2}3d_{3/2}(3)1s$ | $3p3d(^3P)1s\ ^4P_{5/2}$ |
| $3d_{3/2}3d_{3/2}(2)1s$ | $3d^2(^3F)1s\ ^4F_{5/2}$ | $3p_{3/2}3d_{5/2}(2)1s$ | $3p3d(^1D)1s\ ^2D_{5/2}$ |
| $3d_{3/2}3d_{5/2}(2)1s$ | $3d^2(^3F)1s\ ^2F_{5/2}$ | $3p_{3/2}3d_{5/2}(3)1s$ | $3p3d(^1F)1s\ ^2F_{5/2}$ |
| $3d_{3/2}3d_{5/2}(3)1s$ | $3d^2(^3P)1s\ ^4P_{5/2}$ | | |
| $3d_{5/2}3d_{5/2}(2)1s$ | $3d^2(^1D)1s\ ^2D_{5/2}$ | $3p_{1/2}3d_{5/2}(3)1s$ | $3p3d(^3F1s\ ^4F_{7/2}$ |
| | | $3p_{3/2}3d_{3/2}(3)1s$ | $3p3d(^3F)1s\ ^2F_{7/2}$ |
| $3s_{1/2}3d_{5/2}(3)1s$ | $3s3d(^3D)1s\ ^4D_{7/2}$ | $3p_{3/2}3d_{5/2}(3)1s$ | $3p3d(^3D)1s\ ^4D_{7/2}$ |
| $3d_{3/2}3d_{5/2}(4)1s$ | $3d^2(^3F)1s\ ^2F_{7/2}$ | $3p_{3/2}3d_{5/2}(4)1s$ | $3p3d(^1F)1s\ ^2F_{7/2}$ |
| $3d_{3/2}3d_{5/2}(3)1s$ | $3d^2(^3F)1s\ ^4F_{7/2}$ | | |
| $3d_{5/2}3d_{5/2}(4)1s$ | $3d^2(^1G)1s\ ^2G_{7/2}$ | $3p_{3/2}3d_{5/2}(4)1s$ | $3p3d(^3F)1s\ ^4F_{9/2}$ |
| $3d_{3/2}3d_{5/2}(4)1s$ | $3d^2(^3F)1s\ ^4F_{9/2}$ | | |
| $3d_{5/2}3d_{5/2}(4)1s$ | $3d^2(^1G)1s\ ^2G_{9/2}$ | | |

**Table 2.** Second-order contributions to the energy matrices (a.u.) in the case of Li-like iron, $Z = 26$. Two-particle and three-particle second-order Coulomb contributions are given in columns labelled $E_2^{(2)}$ and $E_3^{(2)}$, respectively.

| $2l_1j_1 2l_2j_2(J_{12})1s$ | $2l_3j_3 2l_4j_4(J_{34})1s$ | $E_2^{(2)}$ | $E_3^{(2)}$ | $B_2^{(2)}$ | $B_3^{(2)}$ |
|---|---|---|---|---|---|
| Odd-parity states, $J = 1/2$ | | | | | |
| $2s_{1/2}2p_{1/2}(0)1s$ | $2s_{1/2}2p_{1/2}(0)1s$ | −0.193825 | −0.106398 | −0.003731 | −0.001018 |
| $2s_{1/2}2p_{1/2}(1)1s$ | $2s_{1/2}2p_{1/2}(1)1s$ | −0.237561 | −0.124665 | −0.009566 | −0.001935 |
| $2s_{1/2}2p_{3/2}(1)1s$ | $2s_{1/2}2p_{3/2}(1)1s$ | −0.253589 | −0.119031 | −0.003277 | −0.000774 |
| $2s_{1/2}2p_{1/2}(0)1s$ | $2s_{1/2}2p_{1/2}(1)1s$ | −0.042755 | −0.012340 | 0.000541 | −0.000041 |
| $2s_{1/2}2p_{1/2}(1)1s$ | $2s_{1/2}2p_{1/2}(0)1s$ | −0.042755 | −0.012340 | 0.000541 | 0.000182 |
| $2s_{1/2}2p_{1/2}(0)1s$ | $2s_{1/2}2p_{3/2}(1)1s$ | −0.034748 | −0.004426 | 0.001354 | 0.000526 |
| $2s_{1/2}2p_{3/2}(1)1s$ | $2s_{1/2}2p_{1/2}(0)1s$ | −0.034403 | −0.004524 | 0.001338 | 0.000219 |
| $2s_{1/2}2p_{1/2}(1)1s$ | $2s_{1/2}2p_{3/2}(1)1s$ | 0.012480 | 0.008471 | 0.001165 | 0.000217 |
| $2s_{1/2}2p_{3/2}(1)1s$ | $2s_{1/2}2p_{1/2}(1)1s$ | 0.012331 | 0.008551 | 0.001154 | 0.000131 |
| Odd-parity states, $J = 3/2$ | | | | | |
| $2s_{1/2}2p_{1/2}(1)1s$ | $2s_{1/2}2p_{1/2}(1)1s$ | −0.206146 | −0.108680 | −0.000779 | 0.000136 |
| $2s_{1/2}2p_{3/2}(1)1s$ | $2s_{1/2}2p_{3/2}(1)1s$ | −0.227394 | −0.121216 | −0.003354 | −0.000897 |
| $2s_{1/2}2p_{3/2}(2)1s$ | $2s_{1/2}2p_{3/2}(2)1s$ | −0.248060 | −0.117944 | −0.005786 | −0.001151 |
| $2s_{1/2}2p_{1/2}(1)1s$ | $2s_{1/2}2p_{3/2}(1)1s$ | 0.042573 | 0.012163 | −0.000008 | −0.000136 |
| $2s_{1/2}2p_{3/2}(1)1s$ | $2s_{1/2}2p_{1/2}(1)1s$ | 0.042124 | 0.012327 | −0.000005 | 0.000214 |
| $2s_{1/2}2p_{1/2}(1)1s$ | $2s_{1/2}2p_{3/2}(2)1s$ | −0.038850 | −0.004963 | 0.001514 | 0.000243 |
| $2s_{1/2}2p_{3/2}(2)1s$ | $2s_{1/2}2p_{1/2}(1)1s$ | −0.038463 | −0.005073 | 0.001495 | 0.000615 |
| $2s_{1/2}2p_{3/2}(1)1s$ | $2s_{1/2}2p_{3/2}(2)1s$ | −0.020468 | −0.010156 | −0.002047 | −0.000310 |
| $2s_{1/2}2p_{3/2}(2)1s$ | $2s_{1/2}2p_{3/2}(1)1s$ | −0.020468 | −0.010156 | −0.002047 | −0.000753 |
| Odd-parity states, $J = 5/2$ | | | | | |
| $2s_{1/2}2p_{3/2}(2)1s$ | $2s_{1/2}2p_{3/2}(2)1s$ | −0.151553 | −0.095671 | −0.000630 | 0.000043 |
| Even-parity states, $J = 1/2$ | | | | | |
| $2s_{1/2}2s_{1/2}(0)1s$ | $2s_{1/2}2s_{1/2}(0)1s$ | −0.170297 | −0.096618 | −0.003247 | −0.000927 |
| $2p_{1/2}2p_{1/2}(0)1s$ | $2p_{1/2}2p_{1/2}(0)1s$ | −0.262073 | −0.160578 | −0.005715 | −0.001918 |
| $2p_{3/2}2p_{3/2}(0)1s$ | $2p_{3/2}2p_{3/2}(0)1s$ | −0.277998 | −0.171339 | −0.005030 | −0.002463 |
| $2p_{1/2}2p_{3/2}(1)1s$ | $2p_{1/2}2p_{3/2}(1)1s$ | −0.276600 | −0.155257 | −0.003743 | −0.001676 |
| $2s_{1/2}2s_{1/2}(0)1s$ | $2p_{1/2}2p_{1/2}(0)1s$ | 0.017788 | 0.011430 | 0.000579 | 0.000415 |
| $2p_{1/2}2p_{1/2}(0)1s$ | $2s_{1/2}2s_{1/2}(0)1s$ | 0.017788 | 0.011430 | 0.000579 | 0.000071 |
| $2s_{1/2}2s_{1/2}(0)1s$ | $2p_{3/2}2p_{3/2}(0)1s$ | 0.025993 | 0.016993 | 0.001037 | 0.000584 |
| $2p_{3/2}2p_{3/2}(0)1s$ | $2s_{1/2}2s_{1/2}(0)1s$ | 0.025628 | 0.017438 | 0.001022 | 0.000509 |
| $2s_{1/2}2s_{1/2}(0)1s$ | $2p_{1/2}2p_{3/2}(1)1s$ | 0.000000 | −0.000064 | 0.000000 | 0.000188 |
| $2p_{1/2}2p_{3/2}(1)1s$ | $2s_{1/2}2s_{1/2}(0)1s$ | 0.000000 | −0.000065 | 0.000000 | −0.000078 |
| $2p_{1/2}2p_{1/2}(0)1s$ | $2p_{3/2}2p_{3/2}(0)1s$ | −0.033784 | −0.021423 | −0.001274 | −0.000570 |
| $2p_{3/2}2p_{3/2}(0)1s$ | $2p_{1/2}2p_{1/2}(0)1s$ | −0.033135 | −0.022070 | −0.001256 | −0.000628 |
| $2p_{1/2}2p_{1/2}(0)1s$ | $2p_{1/2}2p_{3/2}(1)1s$ | −0.049142 | −0.014321 | 0.001915 | 0.000436 |
| $2p_{1/2}2p_{3/2}(1)1s$ | $2p_{1/2}2p_{1/2}(0)1s$ | −0.048652 | −0.014509 | 0.001892 | 0.000372 |
| $2p_{3/2}2p_{3/2}(0)1s$ | $2p_{1/2}2p_{3/2}(1)1s$ | 0.034403 | 0.010135 | −0.001338 | −0.000251 |
| $2p_{1/2}2p_{3/2}(1)1s$ | $2p_{3/2}2p_{3/2}(0)1s$ | 0.034748 | 0.010005 | −0.001354 | −0.000305 |
| Even-parity states, $J = 3/2$ | | | | | |
| $2p_{1/2}2p_{3/2}(1)1s$ | $2p_{1/2}2p_{3/2}(1)1s$ | −0.213379 | −0.136514 | −0.004289 | −0.001621 |
| $2p_{1/2}2p_{3/2}(2)1s$ | $2p_{1/2}2p_{3/2}(2)1s$ | −0.285911 | −0.161537 | −0.007264 | −0.001454 |
| $2p_{3/2}2p_{3/2}(2)1s$ | $2p_{3/2}2p_{3/2}(2)1s$ | −0.287856 | −0.158846 | −0.004584 | −0.001365 |
| $2p_{1/2}2p_{3/2}(1)1s$ | $2p_{1/2}2p_{3/2}(2)1s$ | 0.027333 | 0.007988 | −0.002652 | −0.000689 |
| $2p_{1/2}2p_{3/2}(2)1s$ | $2p_{1/2}2p_{3/2}(1)1s$ | 0.027333 | 0.007988 | −0.002652 | −0.000781 |

**Table 2.** (*concluded*).

| $2l_1j_1 2l_2j_2(J_{12})1s$ | $2l_3j_3 2l_4j_4(J_{34})1s$ | $E_2^{(2)}$ | $E_3^{(2)}$ | $B_2^{(2)}$ | $B_3^{(2)}$ |
|---|---|---|---|---|---|
| Even-parity states, $J = 3/2$ | | | | | |
| $2p_{1/2}2p_{3/2}(1)1s$ | $2p_{3/2}2p_{3/2}(2)1s$ | −0.038850 | −0.011127 | 0.001514 | 0.000329 |
| $2p_{3/2}2p_{3/2}(2)1s$ | $2p_{1/2}2p_{3/2}(1)1s$ | −0.038463 | −0.011273 | 0.001495 | 0.000339 |
| $2p_{1/2}2p_{3/2}(2)1s$ | $2p_{3/2}2p_{3/2}(2)1s$ | 0.008210 | −0.000165 | −0.001651 | −0.000593 |
| $2p_{3/2}2p_{3/2}(2)1s$ | $2p_{1/2}2p_{3/2}(2)1s$ | 0.008166 | −0.000177 | −0.001634 | −0.000564 |
| Even-parity states, $J = 5/2$ | | | | | |
| $2p_{1/2}2p_{3/2}(2)1s$ | $2p_{1/2}2p_{3/2}(2)1s$ | −0.251115 | −0.150760 | −0.001327 | 0.000520 |
| $2p_{3/2}2p_{3/2}(2)1s$ | $2p_{3/2}2p_{3/2}(2)1s$ | −0.217774 | −0.138230 | −0.002071 | −0.000382 |
| $2p_{1/2}2p_{3/2}(2)1s$ | $2p_{3/2}2p_{3/2}(2)1s$ | −0.041945 | −0.014365 | 0.000303 | −0.000008 |
| $2p_{3/2}2p_{3/2}(2)1s$ | $2p_{1/2}2p_{3/2}(2)1s$ | −0.041490 | −0.014565 | 0.000296 | −0.000047 |

**Fig. 2.** (*a*) Second-order Coulomb and (*b*) Breit energy contributions to diagonal matrix elements in Li-like ions.

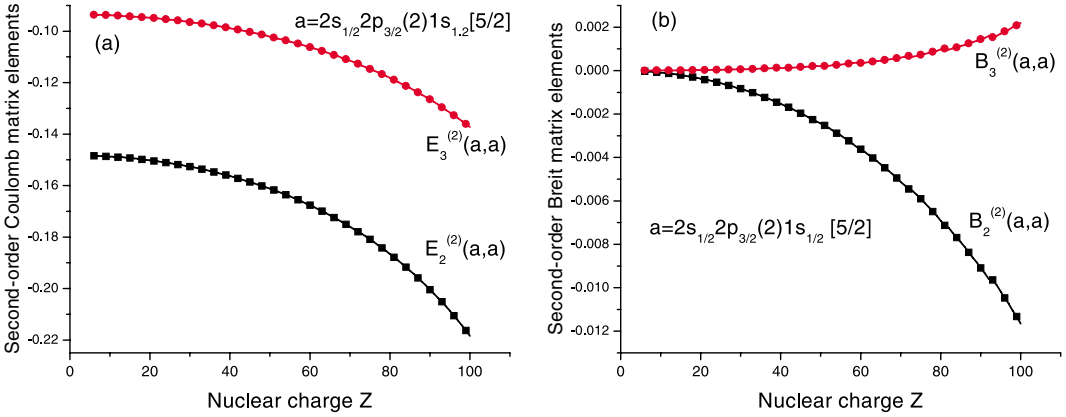


Similarly, for the three-particle contribution we obtain

$$E_3^{(2)}(a,a) = -0.093573 - 0.058Z^2\alpha^2 + \cdots \tag{4}$$

Additional values for terms proportional to $(\alpha Z)^2$ are found from (2). For example, for the diagonal matrix element presented in Fig. 2*b* we obtain

$$B_2^{(2)}(a,a) = -0.018Z^2\alpha^2 + \cdots \tag{5}$$

$$B_3^{(2)}(a,a) = 0.0012Z^2\alpha^2 + \cdots \tag{6}$$

As a result, we can find for the second-order correction

$$E_2^{(2)}(a,a) + E_3^{(2)}(a,a) + B_2^{(2)}(a,a) + B_3^{(2)}(a,a) = -0.243667 - 0.170Z^2\alpha^2 + \cdots \tag{7}$$

for $a = 2s_{1/2}2p_{3/2}(2)1s[5/2]$. The second term in (7) is defined as the second-order relativistic correction and has not previously been calculated.

In Figs. 3*a* and 3*b*, we illustrate the Coulomb $E_2^{(2)}$ and $E_3^{(2)}$ contributions together with the Breit $B_2^{(2)}$ and $B_3^{(2)}$ contributions for the two nondiagonal elements $E_i^{(2)}(a,b)$, $B_i^{(2)}(a,b)$ and $E_2^{(i)}(b,a)$,

**Fig. 3.** (*a*) Second-order Coulomb and (*b*) Breit energy contributions to nondiagonal matrix elements in Li-like ions.

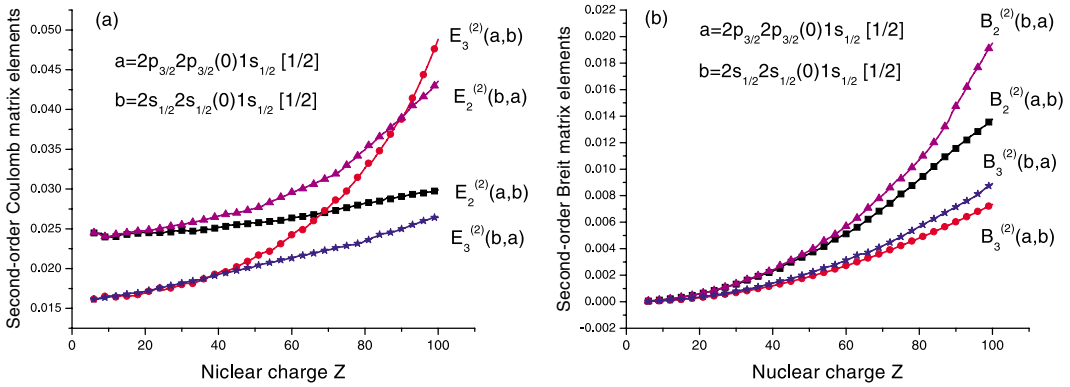


$B_2^{(i)}(b,a)$ for $a = 2p_{3/2}2p_{3/2}(0)1s[1/2]$ and $b = 2s_{1/2}2s_{1/2}(0)1s[1/2]$. We see from Figs. 3*a* and 3*b*, that the ratio of $E_3^{(2)}$ to $E_2^{(2)}$ is about 50% , but the ratio of $B_3^{(2)}$ to $B_2^{(2)}$ is about 20% for both matrix elements. Figure 3*b* illustrates the asymmetry of the nondiagonal matrix elements. The asymmetry of the energy matrix elements in RMBPT calculation is discussed in ref. 12.

In Table 3, we show results for the zeroth-, first-, and second-order Coulomb contributions, $E^{(0)}$, $E^{(1)}$, and $E^{(2)}$ and the first- and second-order Breit–Coulomb corrections, $B^{(1)}$ and $B^{(2)}$. Similar to Table 2, we present the results for the doubly-excited $1s2l2l'$ states for the special case of Li-like iron, $Z = 26$. As one can see from Table 3, the second-order Breit–Coulomb corrections $B^{(2)}$ are smaller than the first-order Breit corrections $B^{(1)}$ by a factor of 10; however, the $B^{(1)}$ is smaller than the first- and second-order Coulomb corrections, $E^{(1)}$ and $E^{(2)}$, by factors 50–100 and 4–7, respectively. It should be noted that the value of the first-order Breit correction $B^{(1)}$ calculated with Dirac functions is different from value of the first-order Breit correction $B_{NR}^{(1)}$ calculated with Coulomb functions (see, for example ref. 32). To clarify this result, let us represent $E^{(1)}$ and $B^{(1)}$ in an $\alpha Z$ expansion form (see, for example ref. 33)

$$E^{(1)} = ZE_{10} + Z^3\alpha^2 E'_{12} + Z^5\alpha^4 E'_{14} + \cdots \tag{8}$$

$$B^{(1)} = Z^3\alpha^2 B_{12} + Z^5\alpha^4 B_{14} + \cdots \tag{9}$$

The sum of $E'_{12}$ and $B_{12}$ in (8) and (9) gives us $B_{NR}^{(1)}$ calculated with Coulomb functions (or $E_{12}$ in Table 4 of ref. 33).

The ratio of nondiagonal and diagonal matrix elements is smaller for the first-order contributions than for the second-order contributions. Another difference between the first- and second-order contributions is the symmetry properties: the first-order nondiagonal matrix elements are symmetric and the second-order nondiagonal matrix elements are not symmetric. The values of $B^{(2)}[v'w'(J'_{12})u'[J], vw(J_{12})u[J]]$ and $B^{(2)}[vw(J_{12})u[J], v'w'(J'_{12})u'[J]]$ matrix elements differ by 30–50%.

### 2.2. Eigenvalues and eigenvectors for doubly-excited states in Li-like ions

After evaluating the energy matrices, we calculate eigenvalues and eigenvectors for states with given values of $J$ and parity. There are two possible methods to carry out the diagonalization: (*a*) diagonalize the sum of zeroth- and first-order matrices, then calculate the second-order contributions using the resulting eigenvectors; or (*b*) diagonalize the sum of the zeroth-, first-, and second-order matrices together. We choose the first method here.

**Table 3.** Contributions to energy matrices (a.u.) before diagonalization in the case of Li-like iron, $Z = 26$.

| $2l_1j_1 2l_2j_2(J_{12})1s$ | $2l_3j_3 2l_4j_4(J_{34})1s$ | $E^{(0)}$ | $E^{(1)}$ | $B^{(1)}$ | $E^{(2)}$ | $B^{(2)}$ |
|---|---|---|---|---|---|---|
| Odd-parity states, $J = 1/2$ | | | | | | |
| $2s_{1/2}2p_{1/2}(0)1s$ | $2s_{1/2}2p_{1/2}(0)1s$ | −171.080643 | 14.979799 | 0.042307 | −0.300223 | −0.004749 |
| $2s_{1/2}2p_{1/2}(1)1s$ | $2s_{1/2}2p_{1/2}(1)1s$ | −171.080643 | 15.933970 | 0.101898 | −0.362226 | −0.011501 |
| $2s_{1/2}2p_{3/2}(1)1s$ | $2s_{1/2}2p_{3/2}(1)1s$ | −170.302660 | 15.963091 | 0.025948 | −0.372619 | −0.004051 |
| $2s_{1/2}2p_{1/2}(0)1s$ | $2s_{1/2}2p_{1/2}(1)1s$ | 0.000000 | 0.641018 | −0.016443 | −0.055095 | 0.000499 |
| $2s_{1/2}2p_{1/2}(1)1s$ | $2s_{1/2}2p_{1/2}(0)1s$ | 0.000000 | 0.641018 | −0.016443 | −0.055095 | 0.000723 |
| $2s_{1/2}2p_{1/2}(0)1s$ | $2s_{1/2}2p_{3/2}(1)1s$ | 0.000000 | 0.362020 | −0.020392 | −0.039174 | 0.001880 |
| $2s_{1/2}2p_{3/2}(1)1s$ | $2s_{1/2}2p_{1/2}(0)1s$ | 0.000000 | 0.362020 | −0.020392 | −0.038927 | 0.001556 |
| $2s_{1/2}2p_{1/2}(1)1s$ | $2s_{1/2}2p_{3/2}(1)1s$ | 0.000000 | −0.516178 | −0.012372 | 0.020951 | 0.001382 |
| $2s_{1/2}2p_{3/2}(1)1s$ | $2s_{1/2}2p_{1/2}(1)1s$ | 0.000000 | −0.516178 | −0.012372 | 0.020882 | 0.001284 |
| Odd-parity states, $J = 3/2$ | | | | | | |
| $2s_{1/2}2p_{1/2}(1)1s$ | $2s_{1/2}2p_{1/2}(1)1s$ | −171.080643 | 15.269847 | 0.002745 | −0.314825 | −0.000643 |
| $2s_{1/2}2p_{3/2}(1)1s$ | $2s_{1/2}2p_{3/2}(1)1s$ | −170.302660 | 15.855894 | 0.028212 | −0.348610 | −0.004251 |
| $2s_{1/2}2p_{3/2}(2)1s$ | $2s_{1/2}2p_{3/2}(2)1s$ | −170.302660 | 15.637351 | 0.050910 | −0.366003 | −0.006937 |
| $2s_{1/2}2p_{1/2}(1)1s$ | $2s_{1/2}2p_{3/2}(1)1s$ | 0.000000 | −0.829696 | 0.005288 | 0.054736 | −0.000143 |
| $2s_{1/2}2p_{3/2}(1)1s$ | $2s_{1/2}2p_{1/2}(1)1s$ | 0.000000 | −0.829696 | 0.005288 | 0.054451 | 0.000209 |
| $2s_{1/2}2p_{1/2}(1)1s$ | $2s_{1/2}2p_{3/2}(2)1s$ | 0.000000 | 0.404751 | −0.022798 | −0.043813 | 0.001756 |
| $2s_{1/2}2p_{3/2}(2)1s$ | $2s_{1/2}2p_{1/2}(1)1s$ | 0.000000 | 0.404751 | −0.022798 | −0.043536 | 0.002111 |
| $2s_{1/2}2p_{3/2}(1)1s$ | $2s_{1/2}2p_{3/2}(2)1s$ | 0.000000 | 0.430469 | 0.018832 | −0.030625 | −0.002357 |
| $2s_{1/2}2p_{3/2}(2)1s$ | $2s_{1/2}2p_{3/2}(1)1s$ | 0.000000 | 0.430469 | 0.018832 | −0.030625 | −0.002800 |
| Odd-parity states, $J = 5/2$ | | | | | | |
| $2s_{1/2}2p_{3/2}(2)1s$ | $2s_{1/2}2p_{3/2}(2)1s$ | −170.302660 | 14.347223 | 0.006059 | −0.247224 | −0.000587 |
| Even-parity states, $J = 1/2$ | | | | | | |
| $2s_{1/2}2s_{1/2}(0)1s$ | $2s_{1/2}2s_{1/2}(0)1s$ | −171.080395 | 14.474443 | 0.028248 | −0.266915 | −0.004174 |
| $2p_{1/2}2p_{1/2}(0)1s$ | $2p_{1/2}2p_{1/2}(0)1s$ | −171.080891 | 17.229558 | 0.059070 | −0.422651 | −0.007633 |
| $2p_{3/2}2p_{3/2}(0)1s$ | $2p_{3/2}2p_{3/2}(0)1s$ | −169.524926 | 17.443735 | 0.042133 | −0.449337 | −0.007493 |
| $2p_{1/2}2p_{3/2}(1)1s$ | $2p_{1/2}2p_{3/2}(1)1s$ | −170.302909 | 17.091768 | 0.034729 | −0.431857 | −0.005419 |
| $2s_{1/2}2s_{1/2}(0)1s$ | $2p_{1/2}2p_{1/2}(0)1s$ | 0.000000 | −0.767134 | −0.002828 | 0.029218 | 0.000995 |
| $2p_{1/2}2p_{1/2}(0)1s$ | $2s_{1/2}2s_{1/2}(0)1s$ | 0.000000 | −0.767134 | −0.002828 | 0.029218 | 0.000650 |
| $2s_{1/2}2s_{1/2}(0)1s$ | $2p_{3/2}2p_{3/2}(0)1s$ | 0.000000 | −1.090732 | −0.007774 | 0.042985 | 0.001620 |
| $2p_{3/2}2p_{3/2}(0)1s$ | $2s_{1/2}2s_{1/2}(0)1s$ | 0.000000 | −1.090732 | −0.007774 | 0.043065 | 0.001531 |
| $2s_{1/2}2s_{1/2}(0)1s$ | $2p_{1/2}2p_{3/2}(1)1s$ | 0.000000 | 0.000000 | 0.000000 | −0.000064 | 0.000188 |
| $2p_{1/2}2p_{3/2}(1)1s$ | $2s_{1/2}2s_{1/2}(0)1s$ | 0.000000 | 0.000000 | 0.000000 | −0.000065 | −0.000078 |
| $2p_{1/2}2p_{1/2}(0)1s$ | $2p_{3/2}2p_{3/2}(0)1s$ | 0.000000 | 0.646169 | 0.005458 | −0.055207 | −0.001844 |
| $2p_{3/2}2p_{3/2}(0)1s$ | $2p_{1/2}2p_{1/2}(0)1s$ | 0.000000 | 0.646169 | 0.005458 | −0.055205 | −0.001884 |
| $2p_{1/2}2p_{1/2}(0)1s$ | $2p_{1/2}2p_{3/2}(1)1s$ | 0.000000 | 0.511974 | −0.028838 | −0.063462 | 0.002351 |
| $2p_{1/2}2p_{3/2}(1)1s$ | $2p_{1/2}2p_{1/2}(0)1s$ | 0.000000 | 0.511974 | −0.028838 | −0.063161 | 0.002263 |
| $2p_{3/2}2p_{3/2}(0)1s$ | $2p_{1/2}2p_{3/2}(1)1s$ | 0.000000 | −0.362020 | 0.020392 | 0.044538 | −0.001588 |
| $2p_{1/2}2p_{3/2}(1)1s$ | $2p_{3/2}2p_{3/2}(0)1s$ | 0.000000 | −0.362020 | 0.020392 | 0.044753 | −0.001659 |
| Even-parity states, $J = 3/2$ | | | | | | |
| $2p_{1/2}2p_{3/2}(1)1s$ | $2p_{1/2}2p_{3/2}(1)1s$ | −170.302909 | 16.429434 | 0.051234 | −0.349893 | −0.005911 |
| $2p_{1/2}2p_{3/2}(2)1s$ | $2p_{1/2}2p_{3/2}(2)1s$ | −170.302909 | 17.234680 | 0.072831 | −0.447449 | −0.008718 |
| $2p_{3/2}2p_{3/2}(2)1s$ | $2p_{3/2}2p_{3/2}(2)1s$ | −169.524926 | 17.151116 | 0.037997 | −0.446703 | −0.005949 |
| $2p_{1/2}2p_{3/2}(1)1s$ | $2p_{1/2}2p_{3/2}(2)1s$ | 0.000000 | −0.286210 | 0.037216 | 0.035321 | −0.003341 |
| $2p_{1/2}2p_{3/2}(2)1s$ | $2p_{1/2}2p_{3/2}(1)1s$ | 0.000000 | −0.286210 | 0.037216 | 0.035321 | −0.003432 |
| $2p_{1/2}2p_{3/2}(1)1s$ | $2p_{3/2}2p_{3/2}(2)1s$ | 0.000000 | 0.404751 | −0.022798 | −0.049977 | 0.001843 |
| $2p_{3/2}2p_{3/2}(2)1s$ | $2p_{1/2}2p_{3/2}(1)1s$ | 0.000000 | 0.404751 | −0.022798 | −0.049736 | 0.001834 |
| $2p_{1/2}2p_{3/2}(2)1s$ | $2p_{3/2}2p_{3/2}(2)1s$ | 0.000000 | −0.054668 | 0.019897 | 0.008045 | −0.002245 |
| $2p_{3/2}2p_{3/2}(2)1s$ | $2p_{1/2}2p_{3/2}(2)1s$ | 0.000000 | −0.054668 | 0.019897 | 0.007988 | −0.002198 |

**Table 3.** (*concluded*).

| $2l_1j_1 2l_2j_2(J_{12})1s$ | $2l_3j_3 2l_4j_4(J_{34})1s$ | $E^{(0)}$ | $E^{(1)}$ | $B^{(1)}$ | $E^{(2)}$ | $B^{(2)}$ |
|---|---|---|---|---|---|---|
| Even-parity states, $J = 3/2$ | | | | | | |
| $2p_{1/2}2p_{3/2}(2)1s$ | $2p_{3/2}2p_{3/2}(2)1s$ | 0.000000 | −0.054668 | 0.019897 | 0.008045 | −0.002245 |
| $2p_{3/2}2p_{3/2}(2)1s$ | $2p_{1/2}2p_{3/2}(2)1s$ | 0.000000 | −0.054668 | 0.019897 | 0.007988 | −0.002198 |
| Even-parity states, $J = 5/2$ | | | | | | |
| $2p_{1/2}2p_{3/2}(2)1s$ | $2p_{1/2}2p_{3/2}(2)1s$ | −170.302909 | 16.869780 | 0.004247 | −0.401875 | −0.000808 |
| $2p_{3/2}2p_{3/2}(2)1s$ | $2p_{3/2}2p_{3/2}(2)1s$ | −169.524926 | 16.416721 | 0.017458 | −0.356004 | −0.002453 |
| $2p_{1/2}2p_{3/2}(2)1s$ | $2p_{3/2}2p_{3/2}(2)1s$ | 0.000000 | 0.467863 | −0.009536 | −0.056310 | 0.000295 |
| $2p_{3/2}2p_{3/2}(2)1s$ | $2p_{1/2}2p_{3/2}(2)1s$ | 0.000000 | 0.467863 | −0.009536 | −0.056055 | 0.000250 |

**Fig. 4.** Contribution to the energies of (*a*) the $2s2p(^3P)1s\ ^4P_{5/2}$ and (*b*) the $2p^2(^3P)2p\ ^4P_{5/2}$ levels of Li-like ions.

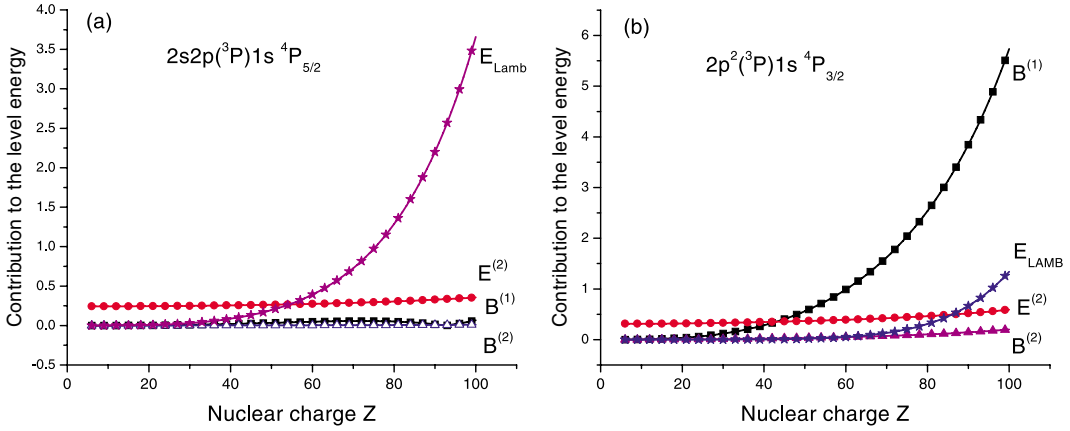


In Table 4, we list the following contributions to the energies of sixteen doubly-excited $1s2l2l'$ states and the ground state in $Fe^{23+}$: $E^{(0+1)} = E^{(0)} + E^{(1)} + B^{(1)}$; the second-order Coulomb energy, $E^{(2)}$; the QED correction, $E_{\rm LAMB}$; and the total theoretical energy, $E_{\rm tot}$, relative to the $1s$ state. The QED correction is approximated as the sum of the one-electron self energy and the first-order vacuum-polarization energy. The screened self-energy and vacuum polarization data given by Johnson and Soff [14] are used to determine the QED correction $E_{\rm LAMB}$. Both $jj$ and LS designations are given in Table 4; however, neither $jj$ nor LS coupling describes the *physical* states properly, except for the single-configuration state $2s_{1/2}2p_{3/2}(2)1s[5/2] \equiv 2s2p(^3P)1s\ ^4P_{5/2}$. We find that the second-order contribution is the largest contribution among the corrections to the $E^{(0+1)}$ value and is equal to about 0.2% of the total energy.

The importance of the second-order contribution to the energies is illustrated in Figs. 4*a* and 4*b*. In these figures, the second-order energy, $E^{(2)}$; the first-order Breit energy, $B^{(1)}$; and the QED contribution, $E_{\rm LAMB}$, are plotted as functions of $Z$ for the doubly-excited $2s2p(^3P)1s\ ^4P_{5/2}$ (Fig. 4*a*) and $2p^2(^3P)1s\ ^4P_{5/2}$ (Fig. 4*b*) states in Li-like ions. We can see from Figs. 4*a* and 4*b* that $E^{(2)}$ is the dominant contribution up to $Z = 54$ and $Z = 42$ for those levels, respectively. In the case of high $Z$, the $E_{\rm LAMB}$ contribution becomes the largest contribution for the $2s2p(^3P)1s\ ^4P_{5/2}$ level and the $B^{(1)}$ contribution becomes the largest one for the $2p^2(^3P)1s\ ^4P_{5/2}$ level. The $E_{\rm LAMB}$ value is smaller than the $E^{(2)}$ value up to $Z = 85$ for the level shown in Fig. 4*b*.

**Fig. 5.** Energies $E/(Z-0.8)^2$ in $10^4$ cm$^{-1}$ of the $1s2l2l'$ levels as functions of $Z$ in Li-like ions.

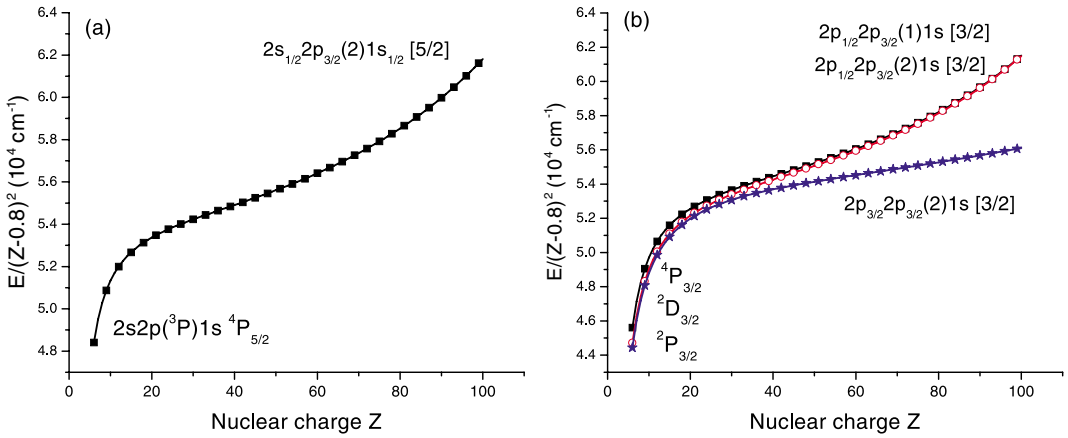


**Fig. 6.** Energies $E/(Z-0.8)^2$ of $1s3l3l'$ states in $10^4$ cm$^{-1}$ as functions of $Z$ in Li-like ions.

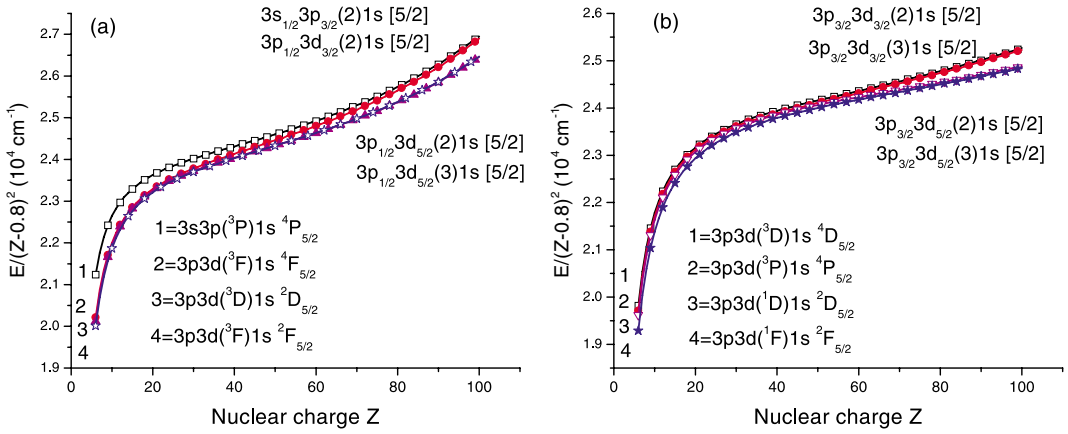


Energies of the $1s2l2l'$ and $1s3l3l'$ states relative to the energy of the $1s$ state and divided by $(Z-0.8)^2$ are plotted in Figs. 5 and 6. It should be noted that $Z$ was decreased by 0.8 to provide better presentation of the energy diagrams. The $Z$ dependence of the odd-parity $2s2p(^3P)1s\ ^4P_{5/2}$ level and the three even-parity $2p^2(^{1,3}L)1s\ ^{2,4}L_{3/2}$ levels is shown in Figs. 5*a* and 5*b*, respectively. The $Z$ dependence of the eight odd-parity $3l3l'(^{1,3}L)1s\ ^{2,4}L_{3/2}$ levels is shown in Fig. 6*a*. We use LS labels for low-$Z$ ions and $jj$ labels for high-$Z$ ions. We see that the energy of all these levels increases sharply with $Z$ for low $Z$ up to $Z = 20$ and then increases slowly for high $Z$ (it is almost constant with $Z$ for $2p_{3/2}2p_{3/2}(2)1s[3/2]$). Comparison of $Z$ dependencies presented in Figs. 5 and 6 shows that energies of the $1s2l2l'$ levels are in the range of 4.8–6.4 in units of $10^4 \times (Z-0.8)^2$ cm$^{-1}$; however, the energies of the $1s3l3l'$ levels are in the range of 1.9–2.7 in units of $10^4 \times (Z-0.8)^2$ cm$^{-1}$.

Strong mixing between states inside of the $1s2l2l'$ odd-parity complex with $J = 1/2$ and 3/2 is discussed in refs. 1 and 2. The $2s_{1/2}2p_{1/2}(1)1s[3/2]$, $2s_{1/2}2p_{3/2}(1)1s[3/2]$, and $2s_{1/2}2p_{3/2}(1)1s[3/2]$ states are mixed with mixing coefficients equal to 0.4–0.7 for the entire isoelectronic sequence. Similar strong mixing is found inside the $1s3l3l'$ odd-parity complex with $J = 1/2$ and 3/2. In addition to the $3s_{1/2}3p_j(J_{12})1s[3/2]$, the complex with $J = 3/2$ includes the $3p_j3d_{j'}(J_{12})1s[3/2]$ states. We found that for the second level of this complex (level labelled $3s3p(^3P)1s\ ^2P_{3/2}$), the contributions

**Table 4.** Energy levels of Li-like iron, $Z = 26$ in a.u., $E^{(0+1)} \equiv E_0 + E_1 + B_1$.

| $jj$-coupling | $E^{(0+1)}$ | $E_2$ | $B_2$ | $E_{\rm LAMB}$ | $E_{\rm tot}$ | $jj$- coupling |
|---|---|---|---|---|---|---|
| $1s^2(^1S)2s\ ^2S_{1/2}$ | −399.323466 | −0.420482 | −0.021942 | 0.160383 | −399.605505 | $1s_{1/2}1s_{1/2}(0)2s$ |
| $2s2p(^3P)1s\ ^4P_{1/2}$ | −156.348260 | −0.253226 | −0.007109 | 0.017003 | −156.591592 | $2s_{1/2}2p_{1/2}(0)1s$ |
| $2s2p(^3P)1s\ ^2P_{1/2}$ | −154.744513 | −0.394425 | −0.006850 | 0.017085 | −155.128702 | $2s_{1/2}2p_{1/2}(1)1s$ |
| $2s2p(^1P)1s\ ^2P_{1/2}$ | −153.895227 | −0.387417 | −0.006342 | 0.018066 | −154.270922 | $2s_{1/2}2p_{3/2}(1)1s$ |
| $2s2p(^3P)1s\ ^4P_{3/2}$ | −156.215283 | −0.255029 | −0.002214 | 0.017313 | −156.455214 | $2s_{1/2}2p_{1/2}(1)1s$ |
| $2s2p(^3P)1s\ ^2P_{3/2}$ | −154.411471 | −0.387204 | −0.003294 | 0.018064 | −154.783905 | $2s_{1/2}2p_{3/2}(1)1s$ |
| $2s2p(^1P)1s\ ^2P_{3/2}$ | −153.785316 | −0.387206 | −0.006323 | 0.018178 | −154.160667 | $2s_{1/2}2p_{3/2}(2)1s$ |
| $2s2p(^1P)1s\ ^4P_{5/2}$ | −155.806401 | −0.247224 | −0.000587 | 0.018318 | −156.035893 | $2s_{1/2}2p_{3/2}(2)1s$ |
| $2s^2(^1S)1s\ ^2S_{1/2}$ | −156.807514 | −0.256840 | −0.003688 | 0.032236 | −157.035806 | $2s_{1/2}2s_{1/2}(0)1s$ |
| $2p^2(^3P)1s\ ^4P_{1/2}$ | −154.123778 | −0.333900 | −0.008340 | 0.000054 | −154.465965 | $2p_{1/2}2p_{1/2}(0)1s$ |
| $2p^2(^3P)1s\ ^2P_{1/2}$ | −152.743760 | −0.485003 | −0.003675 | 0.000306 | −153.232131 | $2p_{3/2}2p_{3/2}(0)1s$ |
| $2p^2(^1S)1s\ ^2S_{1/2}$ | −151.338472 | −0.495017 | −0.009018 | 0.003490 | −151.839017 | $2p_{1/2}2p_{3/2}(1)1s$ |
| $2p^2(^3P)1s\ ^4P_{3/2}$ | −153.827071 | −0.324243 | −0.008277 | 0.000492 | −154.159100 | $2p_{1/2}2p_{3/2}(1)1s$ |
| $2p^2(^1D)1s\ ^2D_{3/2}$ | −152.807675 | −0.449407 | −0.008157 | 0.000490 | −153.264749 | $2p_{1/2}2p_{3/2}(2)1s$ |
| $2p^2(^3P)1s\ ^2P_{3/2}$ | −152.089772 | −0.470393 | −0.004143 | 0.001692 | −152.562616 | $2p_{3/2}2p_{3/2}(2)1s$ |
| $2p^2(^3P)1s\ ^4P_{5/2}$ | −153.605262 | −0.333390 | −0.001618 | 0.000895 | −153.939374 | $2p_{1/2}2p_{3/2}(2)1s$ |
| $2p^2(^3P)1s\ ^2D_{5/2}$ | −152.628410 | −0.424490 | −0.001643 | 0.001355 | −153.053188 | $2p_{3/2}2p_{3/2}(2)1s$ |

from the $3p_{1/2}3d_{3/2}(2)1s[3/2]$ and $3p_{3/2}3d_{5/2}(2)1s[3/2]$ states are important. The odd-parity complex with $J = 5/2$ includes eight states shown in Fig. 6. The first level of this complex $3s3p(^3P)1s\ ^4P_{5/2}$ is defined by the $3s_{1/2}3p_{3/2}(2)1s[5/2]$ state with a small contribution from the $3p_{3/2}3d_{3/2}(3)1s[5/2]$ state for low-$Z$ ions. Two states $3p_{1/2}3d_{3/2}(2)1s[5/2]$ and $3p_{1/2}3d_{3/2}(3)1s[5/2]$ give almost equal contributions to the third, $3p3d(^3D)1s\ ^2D_{5/2}$, and fourth, $3p3d(^3F)1s\ ^2F_{5/2}$, levels of this complex. Mixing between $3s_{1/2}3d_j$ and $3p_j3p_{j'}$ states inside of the even-parity complex for Mg-like ions is discussed in ref. 34. We find similar mixing between $3s_{1/2}3d_j(J_{12})1s$ and $3p_j3p_{j'}(J_{12})1s$ states inside of the even-parity complex with $J = 1/2 - 5/2$ in Li-like ions.

## 3. Comparison of results with theory and experiment

We calculated the energies of the 16 doubly-excited $1s2l2l'$ states, the 63 doubly-excited $1s3l3l'$ states, and the $1s^22p$ and $1s^23l$ singly-excited states together with the ground $1s^22s$ state for Li-like ions with nuclear charges $Z = 6$–100. In Table 5, we illustrate our theoretical results for energies of the $1s^22p$, $1s^23l$, and the 79 doubly-excited $1s2l2l'$ and $1s3l3l'$ states counted from the ground $1s^22s$ state for Li-like Ar, Fe, Kr, and Mo. These ions are most frequently studied experimentally and theoretically (see, for example, refs. 11, 35–40).

### 3.1. Excitation energies of doubly-excited states in Li-like ions

Comparisons of our RMBPT energies with other theoretical and experimental data are too voluminous to include here; therefore, we present several examples of comparisons for selected levels and ions. In Table 6, our theoretical results for the $2s2p(^{1,3}P)1s\ ^4P_J$ and $2s2p(^{1,3}P)1s\ ^2P_J$ levels are compared with available recommended NIST data for $Mg^{9+}$ [16], $Al^{10+}$ [17], $Si^{11+}$ [18], $P^{12+}$ [19], $S^{13+}$ [20], $K^{16+}$ [21], $Ca^{17+}$ [21], $Sc^{18+}$ [21], $Ti^{19+}$ [21], $V^{20+}$ [24], $Cr^{21+}$ [25], $Fe^{23+}$ [27], $Ni^{25+}$ [21], and $Cu^{26+}$ [29]. We see from Table 6 that the difference between our RMBPT results and recommended NIST data is 0.001–0.01%. In Table 7, our theoretical results for the $2s^2(^1S)1s\ ^2S_{1/2}$ level and the eight $2p^2(^{1,3}L)1s\ ^{2,4}L_J$ levels are compared with NIST data. Table 7 is organized in a similar way to Table 6. We can see that our RMBPT results are in excellent agreement with recommended NIST

**Table 5.** Energies ($10^4$ cm$^{-1}$) for the $1s^2nl\ ^2L_J$, $2l2l'(^{1,3}L)1s\ ^{2,4}L_J$, and $3l3l'(^{1,3}L)1s\ ^{2,4}L_J$ levels in Li-like ions given relative to the ground state, $1s^22s\ ^2S_{1/2}$.

| | $Z = 18$ | $Z = 26$ | $Z = 36$ | $Z = 42$ |
|---|---|---|---|---|
| $1s^22p\ ^2P_{1/2}$ | 25.72 | 39.23 | 57.53 | 69.55 |
| $1s^22p\ ^2P_{3/2}$ | 28.28 | 52.11 | 109.94 | 171.15 |
| $1s^23s\ ^2S_{1/2}$ | 417.57 | 926.91 | 1859.84 | 2586.65 |
| $1s^23p\ ^2P_{1/2}$ | 424.68 | 937.80 | 1875.80 | 2605.92 |
| $1s^23p\ ^2P_{3/2}$ | 425.44 | 941.61 | 1891.33 | 2636.06 |
| $1s^23d\ ^2D_{3/2}$ | 428.12 | 945.74 | 1897.18 | 2642.86 |
| $1s^23d\ ^2D_{5/2}$ | 428.35 | 946.94 | 1902.05 | 2652.23 |
| $2s^2(^1S)1s\ ^2S_{1/2}$ | 2483.63 | 5324.07 | 10429.62 | 14352.12 |
| $2s2p(^3P)1s\ ^4P_{1/2}$ | 2490.09 | 5333.82 | 10444.22 | 14370.19 |
| $2s2p(^3P)1s\ ^4P_{3/2}$ | 2490.78 | 5336.81 | 10451.87 | 14380.13 |
| $2s2p(^1P)1s\ ^4P_{5/2}$ | 2492.49 | 5346.02 | 10495.05 | 14469.94 |
| $2s2p(^3P)1s\ ^2P_{1/2}$ | 2510.40 | 5365.93 | 10491.85 | 14427.51 |
| $2s2p(^3P)1s\ ^2P_{3/2}$ | 2511.75 | 5373.49 | 10530.14 | 14509.27 |
| $2s2p(^1P)1s\ ^2P_{1/2}$ | 2519.84 | 5384.75 | 10547.06 | 14530.29 |
| $2s2p(^1P)1s\ ^2P_{3/2}$ | 2520.39 | 5387.17 | 10553.86 | 14540.74 |
| $2p^2(^3P)1s\ ^4P_{1/2}$ | 2518.12 | 5380.47 | 10518.97 | 14461.80 |
| $2p^2(^3P)1s\ ^4P_{3/2}$ | 2519.26 | 5387.21 | 10556.68 | 14545.31 |
| $2p^2(^3P)1s\ ^4P_{5/2}$ | 2520.51 | 5392.03 | 10565.81 | 14555.39 |
| $2p^2(^1D)1s\ ^2D_{3/2}$ | 2532.09 | 5406.84 | 10583.63 | 14576.12 |
| $2p^2(^3P)1s\ ^2D_{5/2}$ | 2532.16 | 5411.48 | 10620.35 | 14659.16 |
| $2p^2(^3P)1s\ ^2P_{1/2}$ | 2534.66 | 5407.55 | 10579.03 | 14568.56 |
| $2p^2(^3P)1s\ ^2P_{3/2}$ | 2537.22 | 5422.25 | 10639.83 | 14683.48 |
| $2p^2(^1S)1s\ ^2S_{1/2}$ | 2549.98 | 5438.13 | 10657.03 | 14701.22 |
| $3s^2(^1S)1s\ ^2S_{1/2}$ | 3367.07 | 7248.87 | 14249.66 | 19644.39 |
| $3s3p(^3P)1s\ ^4P_{1/2}$ | 3368.10 | 7250.40 | 14251.95 | 19647.21 |
| $3s3p(^3P)1s\ ^4P_{3/2}$ | 3368.30 | 7251.28 | 14254.40 | 19650.73 |
| $3s3p(^3P)1s\ ^4P_{5/2}$ | 3368.78 | 7253.89 | 14266.69 | 19676.44 |
| $3s3p(^3P)1s\ ^2P_{1/2}$ | 3373.45 | 7258.91 | 14264.91 | 19663.22 |
| $3s3p(^3P)1s\ ^2P_{3/2}$ | 3373.83 | 7261.20 | 14276.60 | 19688.02 |
| $3s3d(^3D)1s\ ^2D_{3/2}$ | 3374.86 | 7263.62 | 14281.80 | 19694.84 |
| $3s3d(^3D)1s\ ^2D_{5/2}$ | 3374.70 | 7262.95 | 14279.82 | 19691.97 |
| $3s3p(^1P)1s\ ^2P_{1/2}$ | 3376.29 | 7265.05 | 14282.95 | 19696.01 |
| $3s3p(^1P)1s\ ^2P_{3/2}$ | 3376.45 | 7265.58 | 14284.03 | 19697.54 |
| $3p^2(^3P)1s\ ^4P_{1/2}$ | 3376.08 | 7263.90 | 14274.39 | 19675.37 |
| $3p^2(^3P)1s\ ^4P_{3/2}$ | 3376.41 | 7265.78 | 14284.53 | 19698.09 |
| $3p^2(^3P)1s\ ^4P_{5/2}$ | 3376.85 | 7266.62 | 14286.39 | 19701.32 |
| $3s3d(^3D)1s\ ^4D_{1/2}$ | 3376.87 | 7265.98 | 14283.74 | 19696.45 |
| $3s3d(^3D)1s\ ^4D_{3/2}$ | 3376.92 | 7266.25 | 14285.45 | 19700.01 |
| $3s3d(^3D)1s\ ^4D_{5/2}$ | 3377.00 | 7268.11 | 14292.80 | 19711.36 |
| $3s3d(^3D)1s\ ^4D_{7/2}$ | 3377.12 | 7267.21 | 14288.71 | 19705.99 |
| $3p3d(^3F)1s\ ^4F_{3/2}$ | 3379.66 | 7270.52 | 14291.00 | 19705.54 |
| $3p3d(^3F)1s\ ^4F_{5/2}$ | 3379.83 | 7271.00 | 14291.36 | 19705.46 |
| $3p3d(^3F)1s\ ^4F_{7/2}$ | 3380.18 | 7273.06 | 14299.92 | 19721.05 |
| $3p3d(^3F)1s\ ^4F_{9/2}$ | 3380.61 | 7275.47 | 14311.48 | 19745.49 |
| $3s3d(^1D)1s\ ^2D_{3/2}$ | 3380.15 | 7271.25 | 14292.35 | 19707.98 |
| $3s3d(^1D)1s\ ^2D_{5/2}$ | 3380.35 | 7272.32 | 14298.08 | 19719.93 |
| $3p3d(^3D)1s\ ^2D_{3/2}$ | 3380.89 | 7274.60 | 14302.57 | 19721.44 |
| $3p3d(^3D)1s\ ^2D_{5/2}$ | 3380.80 | 7273.98 | 14300.96 | 19722.21 |

**Table 5.** (*concluded*).

| | $Z = 18$ | $Z = 26$ | $Z = 36$ | $Z = 42$ |
|---|---|---|---|---|
| $3p^2(^3P)1s\ ^2P_{1/2}$ | 3380.34 | 7270.97 | 14290.54 | 19704.61 |
| $3p^2(^3P)1s\ ^2P_{3/2}$ | 3380.96 | 7274.09 | 14300.74 | 19720.46 |
| $3p3d(^3F)1s\ ^2F_{5/2}$ | 3382.11 | 7275.78 | 14303.10 | 19723.59 |
| $3p3d(^3F)1s\ ^2F_{7/2}$ | 3382.80 | 7278.62 | 14314.65 | 19745.75 |
| $3p^2(^1S)1s\ ^2S_{1/2}$ | 3382.02 | 7278.79 | 14312.21 | 19742.57 |
| $3p3d(^3D)1s\ ^4D_{1/2}$ | 3383.51 | 7277.25 | 14303.09 | 19721.19 |
| $3p3d(^3D)1s\ ^4D_{3/2}$ | 3383.59 | 7277.52 | 14303.55 | 19723.54 |
| $3p3d(^3D)1s\ ^4D_{5/2}$ | 3383.73 | 7278.24 | 14310.72 | 19740.81 |
| $3p3d(^3D)1s\ ^4D_{7/2}$ | 3383.96 | 7279.72 | 14315.91 | 19750.75 |
| $3p3p(^1D)1s\ ^2D_{5/2}$ | 3384.48 | 7279.39 | 14310.08 | 19737.19 |
| $3p^2(^1D)1s\ ^2D_{3/2}$ | 3384.48 | 7279.49 | 14311.81 | 19741.35 |
| $3p3d(^3P)1s\ ^4P_{1/2}$ | 3385.05 | 7280.99 | 14315.68 | 19746.56 |
| $3p3d(^3P)1s\ ^4P_{3/2}$ | 3385.00 | 7280.81 | 14313.92 | 19744.13 |
| $3p3d(^3P)1s\ ^4P_{5/2}$ | 3384.95 | 7280.94 | 14317.42 | 19750.45 |
| $3p3d(^1D)1s\ ^2D_{3/2}$ | 3386.19 | 7281.86 | 14316.79 | 19748.37 |
| $3p3d(^1D)1s\ ^2D_{5/2}$ | 3386.55 | 7283.69 | 14320.89 | 19754.64 |
| $3p3d(^3P)1s\ ^2P_{1/2}$ | 3387.46 | 7284.60 | 14320.66 | 19752.31 |
| $3p3d(^3P)1s\ ^2P_{3/2}$ | 3387.33 | 7284.34 | 14321.49 | 19755.88 |
| $3d3d(^3F)1s\ ^2F_{5/2}$ | 3387.75 | 7286.18 | 14326.80 | 19763.65 |
| $3d3d(^3F)1s\ ^2F_{7/2}$ | 3387.65 | 7285.97 | 14326.32 | 19762.91 |
| $3d^2(^3F)1s\ ^4F_{3/2}$ | 3387.49 | 7285.24 | 14323.01 | 19755.84 |
| $3d^2(^3F)1s\ ^4F_{5/2}$ | 3387.53 | 7285.25 | 14322.76 | 19755.28 |
| $3d^2(^3F)1s\ ^4F_{7/2}$ | 3388.01 | 7287.28 | 14330.37 | 19769.26 |
| $3d^2(^3F)1s\ ^4F_{9/2}$ | 3387.83 | 7286.91 | 14329.65 | 19768.23 |
| $3p3d(^1F)1s\ ^2F_{7/2}$ | 3390.81 | 7289.71 | 14328.76 | 19764.00 |
| $3p3d(^1F)1s\ ^2F_{5/2}$ | 3390.96 | 7290.26 | 14330.41 | 19766.59 |
| $3d^2(^1G)1s\ ^2G_{7/2}$ | 3391.71 | 7292.48 | 14337.14 | 19778.24 |
| $3d^2(^1G)1s\ ^2G_{9/2}$ | 3391.65 | 7292.28 | 14336.60 | 19777.40 |
| $3d^2(^3P)1s\ ^4P_{1/2}$ | 3391.82 | 7291.77 | 14332.52 | 19767.49 |
| $3d^2(^3P)1s\ ^4P_{3/2}$ | 3391.89 | 7292.16 | 14334.71 | 19772.09 |
| $3d^2(^3P)1s\ ^4P_{5/2}$ | 3391.97 | 7292.44 | 14334.38 | 19771.32 |
| $3d^2(^3P)1s\ ^2P_{1/2}$ | 3392.36 | 7292.65 | 14335.10 | 19772.95 |
| $3d^2(^3P)1s\ ^2P_{3/2}$ | 3392.51 | 7293.12 | 14335.01 | 19772.52 |
| $3d^2(^1D)1s\ ^2D_{5/2}$ | 3394.36 | 7295.58 | 14340.97 | 19783.08 |
| $3d^2(^1D)1s\ ^2D_{3/2}$ | 3394.42 | 7295.80 | 14341.59 | 19783.84 |
| $3p3d(^1P)1s\ ^2P_{1/2}$ | 3395.61 | 7296.24 | 14336.34 | 19771.99 |
| $3p3d(^1P)1s\ ^2P_{3/2}$ | 3395.70 | 7296.69 | 14337.91 | 19774.41 |
| $3d^2(^1S)1s\ ^2S_{1/2}$ | 3404.61 | 7310.95 | 14361.13 | 19804.84 |

data. The $1s3l3l'$ doubly-excited states have received much less attention in the literature than the $1s2l2l'$ states discussed above. A limited number of $1s3l_1\,j_1 3l_2\,j_2 - 1s^2 3l_3\,j_3$ transitions was presented by Beiersdorfer et al. in ref. 37. In Table 8, we compare the RMBPT results with theoretical results and experimental measurements from ref. 37. The theoretical results in ref. 37 were obtained by using the Hebrew University Lawrence Livermore Atomic Code (HULLAC). The difference between RMBPT and HULLAC results is 0.02–0.06%.

### 3.2. Fine structure of the $^2L$ and $^4L$ terms in doubly-excited states of Li-like ions

No direct measurement of fine-structure intervals was made by observing the wavelength differences between transitions within the doublet or quartet states. The intervals of both upper and lower states

**Table 6.** Energies ($10^4$ cm$^{-1}$) of the odd-parity $2l2l'(^{1,3}L)1s\ ^{2,4}L_J$ levels in Li-like ions given relative to the ground state, $1s^2 2s\ ^2S_{1/2}$. Comparison of the RMBPT results with recommended NIST data.

| | $2s2p(^3P)1s$ $^4P_{1/2}$ | $2s2p(^3P)1s$ $^4P_{3/2}$ | $2s2p(^3P)1s$ $^4P_{3/2}$ | $2s2p(^3P)1s$ $^2P_{1/2}$ | $2s2p(^3P)1s$ $^2P_{3/2}$ | $2s2p(^1P)1s$ $^2P_{1/2}$ | $2s2p(^1P)1s$ $^2P_{3/2}$ |
|---|---|---|---|---|---|---|---|
| $Z$=12 | 1064.74 | 1064.84 | 1065.11 | 1076.94 | 1077.16 | 1082.79 | 1082.86 |
| Ref. 16 | 1064.63 | 1064.74 | | 1077.12 | 1077.12 | 1082.90 | 1082.90 |
| $Z$=13 | 1260.62 | 1260.77 | 1261.16 | 1274.13 | 1274.45 | 1280.51 | 1280.63 |
| Ref. 17 | | | 1261.06 | 1274.06 | 1274.38 | 1280.43 | 1280.58 |
| $Z$=14 | 1473.13 | 1473.34 | 1473.89 | 1487.96 | 1488.41 | 1494.90 | 1495.06 |
| Ref. 18 | 1473.23 | 1473.44 | 1473.99 | 1488.09 | 1488.53 | 1495.00 | 1495.21 |
| $Z$=15 | 1702.29 | 1702.60 | 1703.34 | 1718.47 | 1719.07 | 1725.98 | 1726.21 |
| Ref. 19 | 1702.45 | 1702.75 | 1703.50 | 1718.66 | 1719.25 | 1726.13 | 1726.43 |
| $Z$=16 | 1948.15 | 1948.56 | 1949.56 | 1965.69 | 1966.49 | 1973.80 | 1974.11 |
| Ref. 20 | 1948.04 | 1948.45 | 1949.44 | 1965.61 | 1966.39 | 1973.68 | 1974.08 |
| $Z$=19 | 2786.25 | 2787.12 | 2789.30 | 2807.97 | 2809.69 | 2818.17 | 2818.86 |
| Ref. 21 | 2787.10 | 2787.10 | 2787.10 | 2807.90 | 2807.90 | 2818.20 | 2818.20 |
| $Z$=20 | 3099.26 | 3100.34 | 3103.08 | 3122.41 | 3124.59 | 3133.44 | 3134.30 |
| Ref. 21 | | | | | | 3135.20 | 3135.20 |
| $Z$=21 | 3429.16 | 3430.48 | 3433.91 | 3453.76 | 3456.49 | 3465.73 | 3466.78 |
| Ref. 21 | | | | | | 3466.40 | 3466.40 |
| $Z$=22 | 3776.00 | 3777.59 | 3781.83 | 3802.08 | 3805.47 | 3815.09 | 3816.37 |
| Ref. 21 | | | | | | 3816.20 | 3816.20 |
| $Z$=23 | 4139.83 | 4141.73 | 4146.93 | 4167.40 | 4171.58 | 4181.59 | 4183.12 |
| Ref. 24 | | | | 4167.90 | 4171.90 | 4182.00 | 4182.00 |
| $Z$=24 | 4520.70 | 4522.94 | 4529.28 | 4549.77 | 4554.90 | 4565.31 | 4567.12 |
| Ref. 25 | | | | | 4554.80 | 4564.80 | |
| $Z$=26 | 5333.82 | 5336.81 | 5346.02 | 5365.93 | 5373.49 | 5384.75 | 5387.17 |
| Ref. 27 | 5328.79 | 5339.00 | | 5365.70 | 5375.20 | 5384.40 | 5390.30 |
| $Z$=28 | 6215.83 | 6219.68 | 6232.72 | 6251.00 | 6261.91 | 6274.11 | 6277.24 |
| Ref. 21 | 6219.80 | 6222.80 | | 6251.60 | 6261.70 | 6275.50 | |
| $Z$=29 | 6682.83 | 6687.14 | 6702.54 | 6719.55 | 6732.53 | 6745.25 | 6748.76 |
| Ref. 29 | | | 6702.00 | | | | |

**Note:** Ref. 16, $Mg^{9+}$; Ref. 17, $Al^{10+}$; Ref. 18, $Si^{11+}$; Ref. 19, $P^{12+}$; Ref. 20, $S^{13+}$; Ref. 21, $K^{16+}$; Ref. 21, $Ca^{17+}$; Ref. 21, $Sc^{18+}$; Ref. 21, $Ti^{19+}$; Ref. 24, $V^{20+}$; Ref. 25, $Cr^{21+}$; Ref. 27, $Fe^{23+}$; Ref. 21, $Ni^{25+}$; and Ref. 29, $Cu^{26+}$.

are determined if all allowed transitions are observed [41, 42]. In Table 9, we show results for the fine-structure splitting of the $1s2s2p\ ^4P$ and the $1s2p^2\ ^4P$ terms for Li-like ions with $Z = 6$–8. Our RMBPT results are compared with experimental measurements from ref. 41 and the theoretical data obtained using the MZ code [2]. This code is based on the $Z$-expansion of nonreativistic energy matrix with the addition of the relativistic Breit correction (see refs. 1 and 2 for details).

The fine-structure intervals are quite regular throughout the isoelectronic sequence, as seen from Figs. 7 and 8. In Figs. 7 and 8, we present the fine-structure splitting divided by $(Z - 0.8)^3$ for the doublet and quartet terms of the $1s2l2l'$ and $1s3l3l'$ states. It should be noted that energy splitting $E$ was divided by $(Z - 0.8)^3$ to provide a better presentation of the energy diagrams. The energy difference between the $^4P_{3/2}$ and $^4P_{1/2}$ levels in the $2s2p(^3P)1s\ ^4P_J$ quartet term is very small, as shown in Fig. 7*a*; however, the energy difference between the $^4P_{5/2}$ and $^4P_{3/2}$ levels rapidly increases with increasing $Z$. Similar behavior is found for the $3s3p(^3P)1s\ ^4P_J$ quartet term shown in Fig. 8*a*.

**Table 7.** Energies ($10^4$ cm$^{-1}$) of the even-parity $2l2l'(^{1,3}L)1s\ ^{2,4}L_J$ levels in Li-like ions given relative to the ground state, $1s^22s\ ^2S_{1/2}$. Comparison of the RMBPT results with recommended NIST data.

| | $2s^2(^1S)1s$ $^2S_{1/2}$ | $2p^2(^3P)1s$ $^4P_{1/2}$ | $2p^2(^3P)1s$ $^2P_{1/2}$ | $2p^2(^1S)1s$ $^2S_{1/2}$ | $2p^2(^3P)1s$ $^4P_{3/2}$ | $2p^2(^1D)1s$ $^2D_{3/2}$ | $2p^2(^3P)1s$ $^2P_{3/2}$ | $2p^2(^3P)1s$ $^4P_{5/2}$ | $2p^2(^1D)1s$ $^2D_{5/2}$ |
|---|---|---|---|---|---|---|---|---|---|
| $Z$=12 | 1060.48 | 1081.84 | 1091.67 | 1100.88 | 1082.03 | 1089.58 | 1092.06 | 1082.23 | 1089.46 |
| Ref. 16 | | 1081.67 | | 1100.80 | 1081.85 | 1089.40 | | 1082.05 | 1089.40 |
| $Z$=13 | 1256.00 | 1279.41 | 1290.35 | 1300.44 | 1279.67 | 1288.09 | 1290.91 | 1279.97 | 1287.99 |
| Ref. 17 | | 1279.25 | 1290.17 | 1300.29 | 1279.51 | 1287.96 | 1290.72 | 1279.80 | 1287.85 |
| $Z$=14 | 1468.15 | 1493.65 | 1505.71 | 1516.72 | 1494.02 | 1503.32 | 1506.49 | 1494.44 | 1503.20 |
| Ref. 18 | 1468.28 | 1493.68 | 1505.72 | 1516.76 | 1494.04 | 1503.38 | 1506.50 | 1494.45 | 1503.38 |
| $Z$=15 | 1696.95 | 1724.61 | 1737.77 | 1749.76 | 1725.10 | 1735.28 | 1738.85 | 1725.67 | 1735.17 |
| Ref. 19 | 1697.13 | 1724.70 | 1737.85 | 1749.85 | 1725.19 | 1735.31 | 1735.42 | 1725.75 | 1735.42 |
| $Z$=16 | 1942.45 | 1972.31 | 1986.59 | 1999.61 | 1972.97 | 1984.03 | 1988.05 | 1973.73 | 1983.95 |
| Ref. 20 | 1942.20 | 1972.13 | 1973.68 | 1999.42 | 1972.79 | 1983.82 | 1987.85 | 1973.53 | 1983.90 |
| $Z$=19 | 2779.40 | 2816.33 | 2834.01 | 2850.62 | 2817.79 | 2831.52 | 2837.32 | 2819.35 | 2831.72 |
| Ref. 21 | | 2816.00 | 2838.40 | 2851.10 | 2816.00 | 2831.80 | 2838.40 | | 2832.10 |
| $Z$=20 | 3092.00 | 3131.45 | 3150.31 | 3168.34 | 3133.31 | 3147.92 | 3154.55 | 3135.24 | 3148.35 |
| Ref. 21 | | | | | | 3148.40 | 3155.10 | | 3148.60 |
| $Z$=21 | 3421.50 | 3463.56 | 3483.61 | 3503.22 | 3465.90 | 3481.38 | 3488.97 | 3468.22 | 3482.13 |
| Ref. 21 | | | 3486.00 | 3504.70 | | 3484.00 | 3486.00 | | 3484.00 |
| $Z$=22 | 3767.93 | 3812.69 | 3833.98 | 3855.33 | 3815.61 | 3831.95 | 3840.67 | 3818.38 | 3833.14 |
| Ref. 21 | | | | 3855.00 | | 3831.90 | 3841.60 | | 3832.90 |
| $Z$=23 | 4131.34 | 4178.89 | 4201.48 | 4224.78 | 4182.53 | 4199.71 | 4209.76 | 4185.77 | 4201.48 |
| Ref. 24 | 4131.70 | | | 4224.70 | | 4199.70 | 4210.00 | 4185.80 | 4201.70 |
| $Z$=24 | 4511.80 | 4562.22 | 4586.19 | 4611.66 | 4566.71 | 4584.72 | 4596.31 | 4570.46 | 4587.24 |
| Ref. 25 | | | | | | 4584.90 | | | 4587.00 |
| $Z$=26 | 5324.07 | 5380.47 | 5407.55 | 5438.13 | 5387.21 | 5406.84 | 5422.25 | 5392.03 | 5411.48 |
| Ref. 27 | 5323.56 | 5380.60 | 5407.70 | 5438.50 | 5387.70 | 5407.00 | 5424.40 | 5393.70 | 5412.60 |
| $Z$=28 | 6205.18 | 6267.88 | 6298.76 | 6335.63 | 6277.78 | 6298.97 | 6319.35 | 6283.67 | 6306.80 |
| Ref. 21 | | 6269.70 | 6299.70 | 6239.70 | 6278.30 | 6300.80 | 6321.00 | | 6308.50 |

**Note:** Ref. 16, $Mg^{9+}$; Ref. 17, $Al^{10+}$; Ref. 18, $Si^{11+}$; Ref. 19, $P^{12+}$; Ref. 20, $S^{13+}$; Ref. 21, $K^{16+}$; Ref. 21, $Ca^{17+}$; Ref. 21, $Sc^{18+}$; Ref. 21, $Ti^{19+}$; Ref. 24, $V^{20+}$; Ref. 25, $Cr^{21+}$; Ref. 27, $Fe^{23+}$; and Ref. 21, $Ni^{25+}$.

The range of energies plotted in Figs. 7*a* and 8*a* differs by a factor of 4. The decrease in the energy range for the fine-structure splitting of $1s3l3l'$ states in comparison with $1s2l2l'$ states is also observed for the doublet terms (compare Figs. 7*b* and 8*b*). The energy difference between the $^2P_{3/2}$ and $^2P_{1/2}$ levels in the $nsnp(^1P)1s\ ^2P_J$ doublet term is very small but the energy difference between the $^2P_{3/2}$ and $^2P_{1/2}$ levels in the $nsnp(^3P)1s\ ^2P_J$ doublet term rapidly increases with increasing $Z$. The energy difference between the $^4P_{5/2}$ and $^4P_{3/2}$ levels in the $2p^2(^3P)1s\ ^4P_J$ quartet term is again very small, as shown in Fig. 7*c*; however, the energy difference between the $^4P_{3/2}$ and $^4P_{1/2}$ levels rapidly increases with increasing $Z$, which is the opposite to the behavior of the $2s2p(^3P)1s\ ^4P_J$ quartet term. Similar behavior of the fine-structure splitting is found for the $3p^2(^3P)1s\ ^4P_J$ quartet term shown in Fig. 8*e*. The unusual splittings are due principally to changes from LS to $jj$ coupling, with mixing from other triplet and singlet states. States with different $J$ complexes mix differently. Further, experimental confirmation would be very helpful in verifying the correctness of these occasionally sensitive mixing parameters.

**Table 8.** Wavelengths λ in Å for $3l3l'(^{1,3}L)1s\ ^2L_J$ - $1s^23l_j$ transitions in $Ar^{15+}$. Comparison with theoretical (HULLAC code) and experimental (Expt.) results from ref. 37.

| LS - designations | | | | | $jj$ - designations | |
|---|---|---|---|---|---|---|
| $3l3l'(^{1,3}L)1s\ ^2L_J$ | $1s^23l\ ^2L_J$ | RMBPT | HULLAC [37] | Expt. [37] | $3l_j3l'_{j'}(J_{12})1s$ | $3l_j$ |
| $3p3d(^1P)1s\ ^2P_{3/2}$ | $1s^23d\ ^2D_{5/2}$ | 3.3700 | 3.3692 | | $3p_{3/2}3d_{5/2}(2)1s$ | $3d_{5/2}$ |
| $3p3d(^1F)1s\ ^2F_{5/2}$ | $1s^23d\ ^2D_{3/2}$ | 3.3751 | 3.3751 | | $3p_{3/2}3d_{5/2}(3)1s$ | $3d_{3/2}$ |
| $3p3d(^1F)1s\ ^2F_{7/2}$ | $1s^23d\ ^2D_{5/2}$ | 3.3756 | 3.3755 | | $3p_{3/2}3d_{5/2}(4)1s$ | $3d_{5/2}$ |
| $3s3p(^3P)1s\ ^2P_{3/2}$ | $1s^23s\ ^2S_{1/2}$ | 3.3827 | 3.3845 | 3.3856 | $3s_{1/2}3p_{3/2}(1)1s$ | $3s_{1/2}$ |
| $3s3p(^3P)1s\ ^2P_{1/2}$ | $1s^23s\ ^2S_{1/2}$ | 3.3831 | 3.3849 | 3.3856 | $3s_{1/2}3p_{1/2}(1)1s$ | $3s_{1/2}$ |
| $3p3d(^3F)1s\ ^2F_{7/2}$ | $1s^23d\ ^2D_{5/2}$ | 3.3847 | 3.3858 | 3.3856 | $3p_{3/2}3d_{3/2}(3)1s$ | $3d_{5/2}$ |
| $3p3d(^3F)1s\ ^2F_{5/2}$ | $1s^23d\ ^2D_{3/2}$ | 3.3852 | 3.3863 | 3.3856 | $3p_{1/2}3d_{5/2}(3)1s$ | $3d_{3/2}$ |
| $3p3d(^3F)1s\ ^2F_{5/2}$ | $1s^23d\ ^2D_{5/2}$ | 3.3855 | 3.3866 | 3.3856 | $3p_{1/2}3d_{5/2}(3)1s$ | $3d_{5/2}$ |
| $3s3d(^3D)1s\ ^2D_{3/2}$ | $1s^23p\ ^2P_{1/2}$ | 3.3896 | 3.3920 | | $3s_{1/2}3d_{3/2}(1)1s$ | $3p_{1/2}$ |
| $3s3d(^3D)1s\ ^2D_{5/2}$ | $1s^23p\ ^2P_{3/2}$ | 3.3907 | 3.3939 | | $3s_{1/2}3d_{3/2}(2)1s$ | $3p_{3/2}$ |
| $3s^2(^1S)1s\ ^2S_{1/2}$ | $1s^23p\ ^2P_{1/2}$ | 3.3986 | 3.4009 | | $3s_{1/2}3s_{1/2}(0)1s$ | $3p_{1/2}$ |
| $3s^2(^1S)1s\ ^2S_{1/2}$ | $1s^23p\ ^2P_{3/2}$ | 3.3995 | 3.4017 | | $3s_{1/2}3s_{1/2}(0)1s$ | $3p_{3/2}$ |

**Table 9.** Fine-structure splitting of the $1s2s2p\ ^4P$ and the $1s2p^2\ ^4P$ terms in $cm^{-1}$ for Li-like ions. Comparison with theoretical results obtained using the MZ code [2] and with experimental measurements from ref. 41.

| | | $1s2s2p\ ^4P$ | | $1s2p^2\ ^4P$ | |
|---|---|---|---|---|---|
| | | $^4P_{5/2}-{}^4P_{3/2}$ | $^4P_{3/2}-{}^4P_{1/2}$ | $^4P_{5/2}-{}^4P_{3/2}$ | $^4P_{3/2}-{}^4P_{1/2}$ |
| $Z=8$ | Expt. | 418±4 | 102±5 | 252±4 | 295±5 |
| | RMBPT | 407 | 102 | 261 | 297 |
| | MZ | 410 | 103 | 242 | 295 |
| $Z=7$ | Expt. | 212±3 | 35±4 | 115±3 | 160±4 |
| | RMBPT | 211 | 39 | 124 | 161 |
| | MZ | 214 | 37 | 109 | 159 |
| $Z=6$ | Expt. | 100±5 | 0±7 | 41±5 | 83±7 |
| | RMBPT | 98 | 8 | 50 | 77 |
| | MZ | 96 | 6 | 37 | 77 |

### 3.3. Excitation energies of singly-excited states in Li-like ions

The energies of $1s^22l$ states are not the subject of this paper as those energies have been studied experimentally and theoretically in numerous publications. For example, the energies of the $1s^22l$ states were calculated using the RMBPT method and all-order method by Johnson et al. in refs. 43–45. The Hylleraas-type variational method was used in ref. 46 to calculate the energies of the lithium $1s^22s\ ^2S$ and $1s^22p\ ^2P$ isoelectronic sequences up to $Z = 20$. There was no previous RMBPT calculation for the energies of the $1s^23l$ states in Li-like ions. We need these data since they are important for the calculation of the $1s3l3l'$–$1s^23l''$ transition energies. These transitions are important for obtaining satellite spectra for the $1s3l$–$1s^2$ lines [37, 38].

We calculate the energies of $1s^23l$ states using two methods. First, we calculate these energies as described above, treating the $1s^23l$ states as a three-electron system. Next, we treat the $1s^23l$ states as a system with one valence electron above the $1s^2$ core as was done in refs. 43–45. As a result, we obtain the energy counted from the energy of the $1s^2$ core, $E(C)$. The sum of the core $E(C)$ energy and the valence $E(nl)$ energies gives us the absolute energy of the three-electron $1s^23l$ system. Comparison

**Fig. 7.** Energy splittings $E/(Z-0.8)^3$ of $1s2l2l'$ states in $cm^{-1}$ as functions of $Z$.

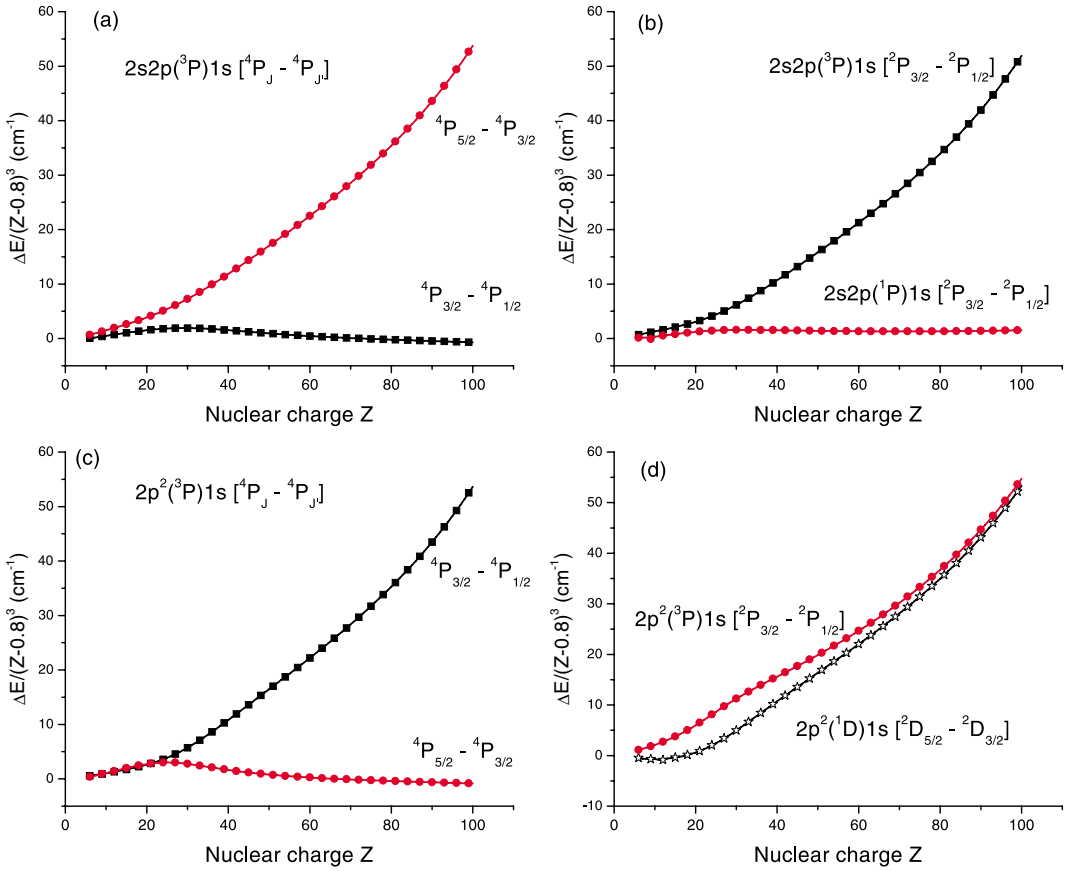


of the results of the $1s^2 3l$ energy obtained by two approaches shows that the difference decreases, as $1/Z$, with increase in $Z$. It is reasonable, since we include additional high-order $1/Z^n$ contributions in RMBPT calculations with the Dirac–Fock functions obtained with the $1s^2$ potential, which are not included in RMBPT calculations with the hydrogenic potential when the $1s^2 3l$ system is treated as a three-electron system.

In Table 10, our theoretical results for the fine-structure splitting of $1s^2 nl\ ^2L$ terms obtained by two methods (with and without $1s^2$ core functions) are compared with available recommended NIST data from refs. 15–31 for Li-like ions with $Z = 6$–42. We can see from Table 10 that our results obtained with the $1s^2$ core functions (hf) are in better agreement with the recommended NIST data than the results obtained with the hydrogenic potential (cl). We use the first set of data in Tables 6 and 7 to present $2l2l'(^{1,3}L)1s\ ^{2,4}L_J$ energies counted from the $1s^2 2s\ ^2S_{1/2}$ ground state. The wavelengths for $3l3l'(^{1,3}L)1s\ ^{2,4}L_J$ - $1s^2 3l\ ^2l_{J'}$ transitions are given in Table 8.

## 4. Conclusion

In conclusion, a systematic second-order RMBPT study of the energies of the doubly-excited states of Li-like ions has been presented. We find that RMBPT gives results in good agreement with experimental and predicted data. It would be beneficial if experimental data for other highly charged Li-like ions were available. At the present time, there are almost no experimental data between $Z = 30$ and 100 for the lithium isoelectronic sequence. Availability of such data could lead to an improved understanding of the

**Table 10.** Splittings of $1s^2nl\ ^2L$ terms in $cm^{-1}$. Comparison of RMBPT data with recommended NIST data. The RMBPT data are calculated with $1s^2$ core (label hf) and without core, as three-electron system (label cl).

| | $2p\ ^2P$ 3/2-1/2 | $3p\ ^2P$ 3/2-1/2 | $3d\ ^2D$ 5/2-3/2 | | $2p\ ^2P$ 3/2-1/2 | $3p\ ^2P$ 3/2-1/2 | $3d\ ^2D$ 5/2-3/2 |
|---|---|---|---|---|---|---|---|
| $Z = 6$ | | | | $Z = 21$ | | | |
| hf | 108 | 32 | 9 | hf | 50671 | 14982 | 4710 |
| cl | 116 | 35 | 16 | cl | 50542 | 14959 | 4741 |
| Ref. 15 | 107 | 31 | 11 | Ref. 23 | 50700 | 15000 | 4000 |
| $Z = 7$ | | | | $Z = 22$ | | | |
| hf | 260 | 76 | 23 | hf | 62166 | 18385 | 5785 |
| cl | 266 | 80 | 30 | cl | 62016 | 18356 | 5819 |
| Ref. 15 | 258 | 74 | 24 | Ref. 21 | 62146 | 18000 | 6000 |
| $Z = 8$ | | | | $Z = 23$ | | | |
| hf | 532 | 156 | 46 | hf | 75527 | 22342 | 7034 |
| cl | 536 | 161 | 56 | cl | 75354 | 22305 | 7072 |
| Ref. 15 | 533 | 157 | 51 | Ref. 24 | 75550 | 22000 | 6600 |
| $Z = 9$ | | | | $Z = 24$ | | | |
| hf | 976 | 287 | 86 | hf | 90952 | 26909 | 8477 |
| cl | 977 | 291 | 97 | cl | 90752 | 26866 | 8517 |
| Ref. 15 | 975 | 282 | 90 | Ref. 25 | 90920 | 26000 | 9000 |
| $Z = 10$ | | | | $Z = 25$ | | | |
| hf | 1651 | 487 | 148 | hf | 108646 | 32150 | 10132 |
| cl | 1648 | 490 | 159 | cl | 108417 | 32098 | 10175 |
| Ref. 15 | 1649 | | | Ref. 21 | 108620 | 30000 | 17000 |
| $Z = 12$ | | | | $Z = 26$ | | | |
| hf | 3981 | 1174 | 360 | hf | 128828 | 38129 | 12017 |
| cl | 3966 | 1176 | 375 | cl | 128568 | 38068 | 12065 |
| Ref. 16 | 3975 | 1310 | 390 | Ref. 27 | 128720 | 39000 | 13000 |
| $Z = 13$ | | | | $Z = 27$ | | | |
| hf | 5799 | 1712 | 528 | hf | 151729 | 44915 | 14156 |
| cl | 5777 | 1712 | 544 | cl | 151433 | 44843 | 14207 |
| Ref. 17 | 5789 | 1750 | 430 | Ref. 28 | 151660 | 44000 | 14000 |
| $Z = 14$ | | | | $Z = 28$ | | | |
| hf | 8181 | 2415 | 747 | hf | 177589 | 52579 | 16569 |
| cl | 8150 | 2413 | 765 | cl | 177254 | 52495 | 16624 |
| Ref. 18 | 8176 | 2390 | 690 | Ref. 22 | 177530 | 60000 | 10000 |
| $Z = 15$ | | | | $Z = 29$ | | | |
| hf | 11229 | 3315 | 1030 | hf | 206663 | 61197 | 19279 |
| cl | 11188 | 3313 | 1049 | cl | 206284 | 61100 | 19339 |
| Ref. 19 | 11226 | 3330 | 990 | Ref. 29 | 206533 | 62000 | 20000 |
| $Z = 164$ | | | | $Z = 36$ | | | |
| hf | 15060 | 4448 | 1386 | hf | 524081 | 155363 | 48683 |
| cl | 15009 | 4443 | 1407 | cl | 523168 | 155115 | 48785 |
| Ref. 20 | 15063 | 4530 | 1420 | Ref. 30 | 523850 | | |
| $Z = 19$ | | | | $Z = 42$ | | | |
| hf | 32547 | 9620 | 3016 | hf | 1016044 | 301485 | 93663 |
| cl | 32455 | 9605 | 3043 | cl | 1014337 | 300995 | 93820 |
| Ref. 21 | 32520 | 14900 | 3200 | Ref. 31 | 1014010 | 300400 | 93850 |
| $Z = 20$ | | | | | | | |
| hf | 40857 | 12078 | 3792 | | | | |
| cl | 40746 | 12059 | 3821 | | | | |
| Ref. 21 | 40861 | 11700 | 3000 | | | | |

**Fig. 8.** Energy splittings $E/(Z-0.8)^3$ of $1s3l3l'$ states in $cm^{-1}$ as functions of $Z$.

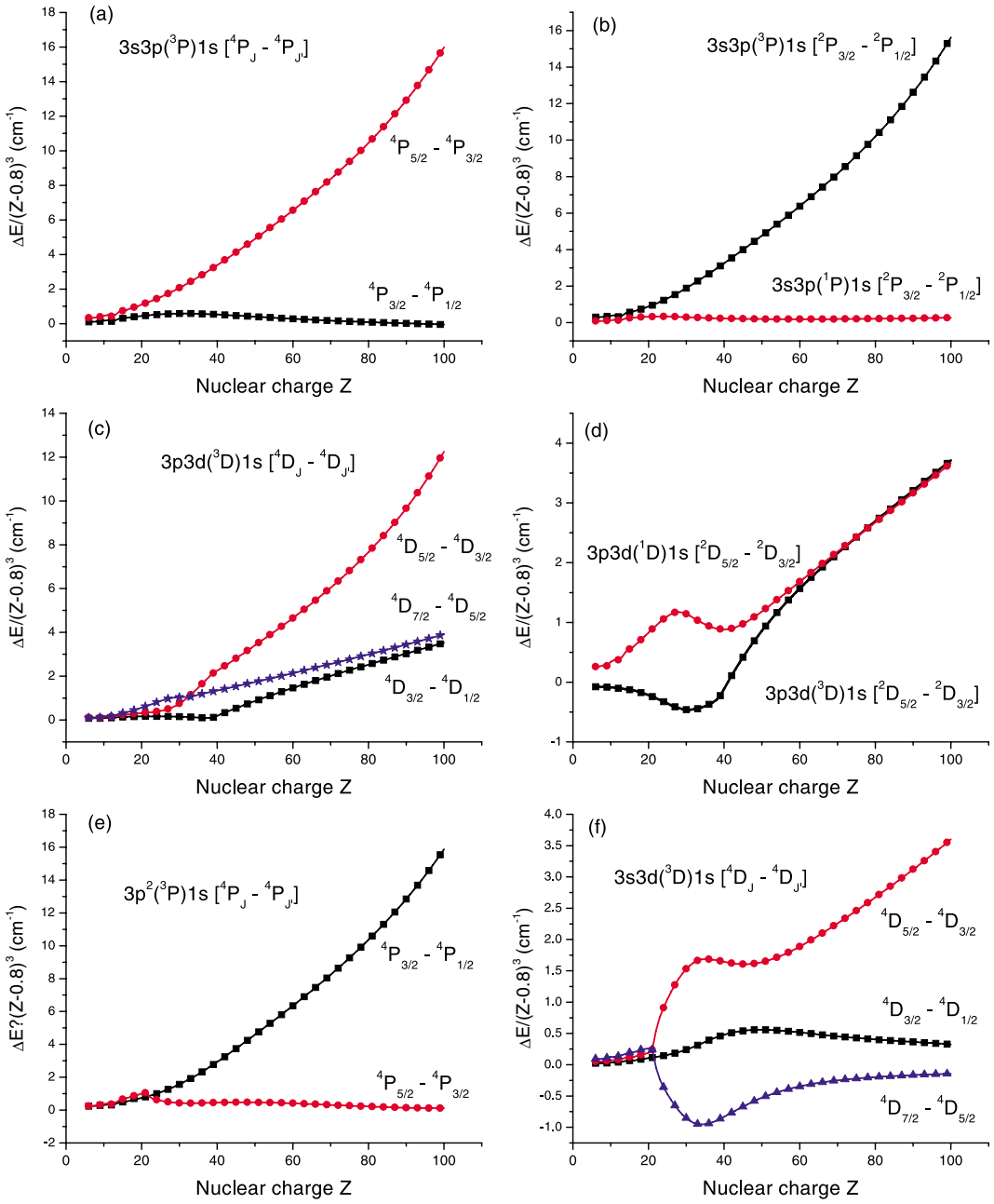


relative importance of different contributions to the energies of highly charged ions. These calculations are presented as a theoretical benchmark for comparison with experiment and theory. The results could be further improved by including third-order correlation corrections.

## Acknowledgments

The work of U.I. Safronova was supported by DOE/NNSA under UNR grant DE-FC52-01NV14050.

## References


1. U.I. Safronova and V.N. Kharitonova. Opt. Spectr. **27**, 300 (1969).
2. L.A. Vainshtein and U.I. Safronova. Atomic Data Nucl. Data Tables, **21**, 49 (1978); **25**, 311 (1980).
3. U.I. Safronova, M.S. Safronova, R. Bruch, and L.A. Vainshtein. Phys. Scripta, **51**, 471 (1995).
4. P. Faucher and J. Dubau. Phys. Rev. A, **31**, 3672 (1985).
5. C.P. Bhalla, A.N. Gabriel, and L.P. Presnyakov. Month. Not. R. Astr. Soc. **172**, 359 (1975).
6. F. Bely-Dubau, A.N. Gabriel, and S. Volonte. Month. Not. R. Astr. Soc. **186**, 405 (1979).
7. M. Bitter, K.W. Hill, M. Zarnstorff, S. von Goeler, R. Hulse, L.C. Johnson, N.R. Sauthoff, S. Sesnic, K.M. Young, M. Tavernier, F. Bely-Dubau, P. Faucher, M. Cornille, and J. Dubau. Phys. Rev. A, **32**, 3011 (1985).
8. M.H. Chen, B. Crasemann, M, Aoyagi, K.N. Huang, and H. Mark. Atomic Data Nucl. Data Tables, **26**, 561 (1981).
9. M.H. Chen. Atomic Data Nucl. Data Tables, **34**, 301 (1986).
10. J. Nilsen. Atomic Data Nucl. Data Tables, **38**, 339 (1988).
11. T. Kato, U.I. Safronova, A.S Shlyaptseva, M. Cornille, J. Dubau, and J. Nilsen. Atomic Data Nucl. Data Tables, **67**, 225 (1997).
12. M.S. Safronova, W.R. Johnson, and U.I. Safronova. Phys. Rev. A, **54**, 2850 (1996).
13. U.I. Safronova, C. Namba, J.R. Albritton, W.R. Johnson, and M.S. Safronova. Phys. Rev. A, **65**, 022507 (2002).
14. W.R. Johnon and G. Soff. At. Data Nucl. Data Tables, **33**, 405 (1985).
15. W.L. Wiese, M.W. Smith, and B.M. Glenon. Atomic Trans. Probabilities, V.1, NSRDS-NBS 4 (1996).
16. V. Kaufman and W.C. Martin. Phys. Chem. Ref. Data, **20**, 83 (1991).
17. V. Kaufman and W.C. Martin. Phys. Chem. Ref. Data, **20**, 775 (1991).
18. W.C. Martin and R. Zalubas. J. Phys. Chem. Ref. Data, **12**, 323 (1983).
19. W.C. Martin, R. Zalubas, and A. Musgrove. J. Phys. Chem. Ref. Data, **14**, 751 (1985).
20. W.C. Martin, R. Zalubas, and A. Musgrove. J. Phys. Chem. Ref. Data, **19**, 821 (1990).
21. J. Shugar and Ch. Corliss. J. Phys. Chem. Ref. Data, **14**, Suppl. 2 (1985).
22. J.R. Fuhr, J.R. Martin, and W.L. Wiese. Corliss, J. Phys. Chem. Ref. Data, **17**, Suppl. 4 (1988).
23. V. Kaufman and J. Sugar. Phys. Chem. Ref. Data, **17**, 1679 (1988).
24. T. Shirai, T. Nakagaki, J. Sugar, and W.L. Wiese. J. Phys. Chem. Ref. Data, **21**, 273 (1992).
25. T. Shirai, Y. Nakai, T. Nakagaki, J. Sugar, and W.L. Wiese. J. Phys. Chem. Ref. Data, **22**, 1279 (1993).
26. T. Shirai, T. Nakagaki, K. Okazaki, J. Sugar, and W.L. Wiese. J. Phys. Chem. Ref. Data, **23**, 179 (1994).
27. T. Shirai, Y. Funatake, K. Mori, J. Sugar, W.L. Wiese, and Y. Nakai. J. Phys. Chem. Ref. Data, **19**, 127 (1990).
28. T. Shirai, A. Mengoni, Y. Nakai, K. Mori, J. Sugar, W.L. Wiese, K. Mori, and N. Sakai. J. Phys. Chem. Ref. Data, **21**, 23 (1992).
29. J. Sugar and A. Musgrove. J. Phys. Chem. Ref. Data, **19**, 527 (1990).
30. T. Shirai, K. Okazaki, and J. Sugar. J. Phys. Chem. Ref. Data, **24**, 1577 (1995).
31. J. Sugar, and A. Musgrove. J. Phys. Chem. Ref. Data, **17**, 155 (1988).
32. V.G. Palchikov and U.I. Safronova. Opt. Spectros. **68**, 281 (1990).
33. U.I. Safronova, W.R. Johnson, and M.S. Safronova. Phys. Scr. A, **58**, 348 (1998).
34. U.I. Safronova, W.R. Johnson, and H.G. Berry. Phys. Rev. A, **61**, 052 503 (2000).
35. V.P. Boiko, S.A. Pikuz, U.I. Safronova, and A.Ya. Faenov. Month. Not. R. Astr. Soc. **185**, 789 (1978).
36. F. Bely-Dubau, J. Dubau, P. Faucher, and A.N. Gabriel. Month. Not. R. Astr. Soc. **198**, 239 (1982).
37. P. Beiersdorfer, A. Osterheld, T.W. Phillips, M. Bitter, K.W. Hill, and S. von Goeler. Phys. Rev. E, **52**, 1980 (1995).
38. A.J. Smith, M. Bitter, H. Hsuan, K.W. Hill, S. von Goeler, J. Timberlake, P. Beiersdorfer, and A. Osterheld. Phys. Rev. A, **47**, 3073 (1993).
39. P. Beiersdorfer, T.W. Phillips, V.L. Jacobs, K.W. Hill, M. Bitter, H. Hsuan, S. von Goeler, and S.M. Kahn. ApJ **409**, 846 (1993).
40. K. Widmann, P. Beiersdorfer, V. Descaux, and M. Bitter. Phys. Rev. A, **53**, 2200 (1996).
41. A.E. Livingston, J.E. Hardis, L.J. Curtis, R.L. Brooks, and H.G. Berry. Phys. Rev. A, **30**, 2089 (1984).
42. E.J. Knystautas and M. Druetta. Phys. Rev. A, **31**, 2279 (1985).

43. W.R. Johnson, M. Idrees, and J. Sapirstein. Phys. Rev. A, **35**, 3218 (1987).
44. W.R. Johnson, A. Blundell, and J. Sapirstein. Phys. Rev. A, **37**, 2764 (1988).
45. A. Blundell, W.R. Johnson, Z.W. Liu, and J. Sapirstein. Phys. Rev. A, **40**, 2233 (1988).
46. Z.-C. Yan, M. Tambasco, and G.W.F. Drake. Phys. Rev. A, **57**, 1652 (1998).
47. M.S. Safronova, W.R. Johnson, and U.I. Safronova. Phys. Rev. A, **53**, 4036 (1996).
48. M.H. Chen, K.T. Cheng, and W.R. Johnson. Phys. Rev. A, **47**, 3692 (1993).
49. U.I. Safronova. Phys. Scr. T, **26**, 59 (1989).

## Appendix A. First- and second-order contributions to energy matrix for $1snln'l'$ states

The model space state vector for a system with three valence electrons can be represented as [12]

$$\Psi_0\left(v_1 w_1\left[J_{12}\right] u_1 J M\right)=\sum_{vwu}\sum_{K''_{12}}\langle vw|K''_{12}\rangle\langle K''_{12}u|K\rangle C_{vv_1ww_1uu_1}\left(J_{12}, J''_{12}, J\right) a_v^\dagger a_w^\dagger a_u^\dagger \tag{A1}$$

where we use the notation $K_i=\{J_i, M_i\}$. The quantity $\langle K_1K_2|K_3\rangle$ is a Clebsch–Gordan coefficient

$$\langle K_1K_2|K_3\rangle=(-1)^{J_1-J_2+M_3}\sqrt{[J_3]}\begin{pmatrix} J_1 & J_2 & J_3 \\ M_1 & M_2 & -M_3\end{pmatrix} \tag{A2}$$

with $[J]=2J+1$. The quantity $C_{vv_1ww_1uu_1}(J_{12}, J''_{12}, J)$ is a symmetry coefficient defined in ref. 12,

$$\begin{aligned} C_{vv_1ww_1uu_1}\left(J_{12}, J''_{12}, J\right)=N\left(v_1w_1\left[J_{12}\right]u_1\right)\Bigg[&\delta\left(u,u_1\right)\delta\left(J_{12},J''_{12}\right)P_{J_{12}}\left(vv_1,ww_1\right)\\ &+\delta\left(u,v_1\right)P_{J''_{12}}\left(vu_1,ww_1\right)\sqrt{\left[J_{12}\right]\left[J''_{12}\right]}\begin{Bmatrix} u_1 & w_1 & J''_{12}\\ v_1 & J & J_{12}\end{Bmatrix}\\ &+(-1)^{v_1+w_1+1+J_{12}}\delta\left(u,w_1\right)P_{J''_{12}}\left(vu_1,wv_1\right)\sqrt{\left[J_{12}\right]\left[J''_{12}\right]}\begin{Bmatrix} u_1 & v_1 & J''_{12}\\ w_1 & J & J_{12}\end{Bmatrix}\Bigg]\end{aligned} \tag{A3}$$

where $N(v_1w_1[J_{12}]u_1)$ is a normalization constant and

$$P_{J_{12}}\left(v_1w_1, vw\right)=\delta_{v_1v}\,\delta_{w_1w}+(-1)^{j_v+j_w+J+1}\,\delta_{w_1v}\,\delta_{v_1w} \tag{A4}$$

Using this representation, it is possible to express the contributions from first-order (see Fig. 1*a*) and second-order (see Fig. 1*b*) RMBPT diagrams to energies of three-electron systems in terms of the contributions of these diagrams to energies of two-electron (heliumlike) ions

$$\begin{aligned} E_2^{(n)}\left(v_1w_1[J_{12}]u_1J, v'_1w'_1[J'_{12}]u'_1J\right)=&\sum_{vwv'w'}\sum_{J''_{12}}E_2^{(n)}\left(vw, v'w', J\right)\eta(vw)\eta\left(v'w'\right)\\ &\times\sum_u C_{vv_1ww_1uu_1}\left(J_{12}, J''_{12}, J\right)C_{v'v'_1w'w'_1uu'_1}\left(J'_{12}, J''_{12}, J\right)\end{aligned} \tag{A5}$$

where $E_2^{(n)}(vw, v'w', J)$ is the two-particle contribution to the $n_v\kappa_v n_w\kappa_w n'_v\kappa'_v n'_w\kappa'_w$ $J$ matrix element for heliumlike ions. Here, $\eta(vw)=1/\sqrt{2}$ if electrons $v$ and $w$ are equivalent and $1/2$ they are not equivalent. This choice accounts for the fact that $E^{(n)}(vw, v'w', J)$ contains both direct and exchange contributions.

The expressions for the two-particle first- and second-order diagram contributions were given in ref. 47

$$E_2^{(1)}\left(vw, v'w', J\right)=Y_J\left(v'w'vw\right) \tag{A6}$$

$$E_2^{(2)}\left(vw, v'w', J\right) = -\sum_{mn}\sum_{k}(-1)^{j_{w'}+j_m+k+J}\left\{\begin{array}{ccc} j_{v'} & j_{w'} & J \\ j_n & j_m & k \end{array}\right\}\frac{X_k(v'w'mn)Y_J(mnvw)}{\varepsilon_{vw}-\varepsilon_{mn}} \tag{A7}$$

Here $\varepsilon_{vw} = \varepsilon_v + \varepsilon_w$, and

$$Y_J(v'w'vw) = \sum_{k}(-1)^{j_{w'}+j_v+k+J}\left\{\begin{array}{ccc} j_{v'} & j_{w'} & J \\ j_w & j_v & k \end{array}\right\}X_k(v'w'vw) + \sum_{k}(-1)^{j_{w'}+j_v+k}\left\{\begin{array}{ccc} j_{v'} & j_{w'} & J \\ j_v & j_w & k \end{array}\right\}X_k(v'w'wv) \tag{A8}$$

where

$$X_k(abcd) = (-1)^k\,\langle a\,\|C_k\|\,c\rangle\,\langle b\,\|C_k\|\,d\rangle\,R_k(abcd) \tag{A9}$$

The radial integral in the above expression is

$$R_k(abcd) = \int_0^\infty r_1^2\,\mathrm{d}r_1\int_0^\infty r_2^2\,\mathrm{d}r_2\frac{r_<^k}{r_>^{k+1}}R_a(r_1)R_b(r_2)R_d(r_2)R_c(r_1) \tag{A10}$$

where $R_a(r_1)$ is a relativistic Dirac–Fock or hydrogenic wave function.

The expressions for the three-particle second-order diagram contributions (Fig. 1*c*) are given in ref. 12

$$\begin{aligned} E_3^{(2)}\left(v_1w_1[J_{12}]u_1J, v_1'w_1'[J_{12}']u_1'J\right) = {} & \sum_{vwu}\sum_{v'w'u'}\sum_{J_{12}''}\sum_{J_{12}'''}\sum_{kk'}(-1)^{j_w+j_w'-j_u-j_u'+J_{12}''+J_{12}'''+k+k'} \\ & \times\sum_n\frac{X_k(vwu'n)X_k(v'w'un)}{\epsilon_n+\epsilon_{u'}-\epsilon_v-\epsilon_w}\sqrt{\left(2J_{12}''+1\right)\left(2J_{12}'''+1\right)} \\ & \times\left\{\begin{array}{ccc} j_n & j_u' & J_{12}'' \\ j_v & j_w & k \end{array}\right\}\left\{\begin{array}{ccc} j_n & j_u & J \\ j_v' & j_w' & k' \end{array}\right\}\left\{\begin{array}{ccc} J_{12}''' & j_u' & J \\ J_{12}'' & j_u & j_n \end{array}\right\} \\ & \times C_{vv_1ww_1uu_1}\left(J_{12}, J_{12}'', J\right)C_{v'v_1'w'w_1'u'u_1'}\left(J_{12}', J_{12}'', J\right) \end{aligned} \tag{A11}$$

We see that the contribution of the *G* diagram is determined by a sum *n* over the single-particle spectrum (with restrictions for states when a denominator is equal to zero).

All of the above expressions were defined for the Coulomb interaction. When we include the Breit interaction in the calculation, the Coulomb matrix element $X_k(ab, cd)$ is modified according to the rule

$$X_k(abcd) \Rightarrow X_k(abcd) + M_k(abcd) + N_k(abcd) \tag{A12}$$

The magnetic radial integrals *M* and *N* are defined by (A.4) and (A.5) of ref. 48.

Let us explain a little more about the difference in calculations of the $1s2l2l'$ and $1s3l3l'$ doubly excited states, also called autoionizing states. The most important difference between autoionization states and other excited states is an additional broadening of levels caused by the decay of these states (e.g., $1s2l2l' \Rightarrow 1s^2kl''$, $1s3l3l' \Rightarrow 1s^2kl''$, $1s2lkl''$). We can rewrite (A7), $E_2^{(2)}(vw, v'w', J)$ in the following way:

$$E_2^{(2)}(vw, v'w', J) = \lim_{\gamma\to 0}\sum_{mn}\sum_{k}(-1)^{j_{w'}+j_m+k+J}\left\{\begin{array}{ccc} j_{v'} & j_{w'} & J \\ j_n & j_m & k \end{array}\right\}\frac{X_k(v'w'mn)Y_J(mnvw)}{\varepsilon_m+\varepsilon_n-\varepsilon_v-\varepsilon_w-i\gamma} \tag{A13}$$

We note that for $1s2l2l'$ states indexes $v$ and $w$ in (A13) can be $v = 2lj$, $w = 2l'j'$, and $n = 1s$ or $m = 1s$. Indexes $m$ or $n$ can include both discrete and continuous excited states. In the case of continuous states, we obtain the same expression as (A13) in ref. 49

$$\lim_{\gamma\to 0}\int_0^\infty \mathrm{d}k \frac{f(2lj2l'j';1skl''j'')}{\varepsilon_{kl''j''}+\varepsilon_{1s}-\varepsilon_{2lj}-\varepsilon_{2l'j'}-i\gamma} = P\int_0^\infty \mathrm{d}k \frac{f(2lj2l'j';1skl''j'')}{\varepsilon_k+\varepsilon_{1s}-\varepsilon_{2lj}-\varepsilon_{2l'j'}} + \frac{i\pi}{k_0} f(2lj2l'j';1sk_0l''j'') \quad \text{(A14)}$$

where $P$ means that the integral must be calculated in the sense of the principal value avoiding the value $\varepsilon_{k_0}+\varepsilon_{1s}-\varepsilon_{2lj}-\varepsilon_{2l'j'}=0$. It should be noted that $k_0=\sqrt{\frac{1}{2}}$ in the hydrogenic approximation.